

Sterile Neutrino Dark Matter in Left-Right Theories

Jeff A. Dror^{1,2} David Dunsky^{1,2} Lawrence J. Hall^{1,2} Keisuke Harigaya³

¹*Department of Physics, University of California, Berkeley, California 94720, USA*

²*Theoretical Physics Group, Lawrence Berkeley National Laboratory, Berkeley, California 94720, USA*

³*School of Natural Sciences, Institute for Advanced Study, Princeton, New Jersey 08540, USA*

ABSTRACT: $SU(2)_L \times SU(2)_R$ gauge symmetry requires three right-handed neutrinos (N_i), one of which, N_1 , can be sufficiently stable to be dark matter. In the early universe, W_R exchange with the Standard Model thermal bath keeps the right-handed neutrinos in thermal equilibrium at high temperatures. N_1 can make up all of dark matter if they freeze-out while relativistic and are mildly diluted by subsequent decays of a long-lived and heavier right-handed neutrino, N_2 . We systematically study this parameter space, constraining the symmetry breaking scale of $SU(2)_R$ and the mass of N_1 to a triangle in the (v_R, M_1) plane, with $v_R = (10^6 - 3 \times 10^{12})$ GeV and $M_1 = (2 \text{ keV} - 1 \text{ MeV})$. Much of this triangle can be probed by signals of warm dark matter, especially if leptogenesis from N_2 decay yields the observed baryon asymmetry. The minimal value of v_R is increased to 10^8 GeV for doublet breaking of $SU(2)_R$, and further to 10^9 GeV if leptogenesis occurs via N_2 decay, while the upper bound on M_1 is reduced to 100 keV. In addition, there is a component of hot N_1 dark matter resulting from the late decay of $N_2 \rightarrow N_1 \ell^+ \ell^-$ that can be probed by future cosmic microwave background observations. Interestingly, the range of v_R allows both precision gauge coupling unification and the Higgs Parity understanding of the vanishing of the Standard Model Higgs quartic at scale v_R . Finally, we study freeze-in production of N_1 dark matter via the W_R interaction, which allows a much wider range of (v_R, M_1) .

Contents

1	Introduction	1
2	Left-right models and neutrino masses	3
3	N_1 stability	5
4	Relativistic freeze-out and dilution	7
5	Signals and future probes	10
5.1	Warmness	10
5.2	Hotness	11
5.3	Early matter dominated era	12
5.4	Leptogenesis	13
6	Predictions on v_R from UV physics	14
6.1	Small Higgs quartic coupling at high energy scales	14
6.2	Gauge coupling unification	15
7	Freeze-In	16
8	Conclusions	17
A	Neutrino mass relations	19
B	A symmetry for the cosmological stability of N_1	26

Contents

1 Introduction

Left-right (LR) symmetry [1–3] is a possible remnant of grand unification [4–7], can restore space-time parity at high energies, solve the strong CP problem [8–12], and explain the small Standard Model (SM) Higgs quartic coupling at high energy scales [12–15]. In LR theories, the electroweak gauge group, $SU(2)_L \times U(1)_Y$, is extended to $SU(2)_L \times SU(2)_R \times U(1)_{B-L}$, which is broken at a scale (v_R) above the weak scale (v), $v_R \gg v$. LR symmetry predicts right-handed neutrinos, which, if their masses and mixing with the left-handed neutrinos are sufficiently small, can be stable. Since right-handed neutrinos are inert under the SM

gauge group, they are candidates to make up the observed dark matter (DM) density of the universe. Right-handed neutrino DM belongs to a class of sterile neutrino DM, and we use “right-handed neutrino” and “sterile neutrino” interchangeably.

How can right-handed neutrino DM be populated in the early universe? For large v_R and/or small reheating temperatures of the universe, production of right-handed neutrinos through the exchange of heavy gauge bosons, W_R and Z_R , is negligible. Right-handed neutrinos can still be produced by their Yukawa coupling with the SM lepton doublets and Higgs [16]. However, this production mechanism is in tension with the constraints from x-ray searches and structure formation of the universe (see e.g. [17]), unless a significant lepton asymmetry is present [18].

Production of right-handed neutrinos by the exchange of W_R and Z_R becomes increasingly effective for higher reheating temperatures. The resultant abundance reproduces the observed DM density for an appropriate reheating temperature; above this temperature, right-handed neutrinos are overproduced.

In the limit of high reheating temperatures, right-handed neutrinos are thermalized via W_R and Z_R exchange. The DM phenomenology of LR theories in the case of high reheat temperatures was first studied in [19], which showed that the lightest right-handed neutrino can make up DM if it decouples while relativistic and has its abundance diluted by decays of heavier right-handed neutrinos into the SM bath through an off-shell W_L via sterile-active mixing. The requirement that the heavier neutrino freezes-out while relativistic leads to a constraint on the W_R mass, $M_{W_R} \gtrsim 10^4$ GeV, with no clear upper bound.

In this work we study the parameter space of LR models systematically, mainly for reheat temperatures after inflation above the temperatures needed to thermalize the right-handed neutrinos by W_R and Z_R exchange. As in [19], right-handed neutrinos decouple relativistically, and the unstable but long-lived states decay to dilute the abundance of the stable state to the observed DM abundance. We extend previous work, finding a bounded parameter space from a combination of constraints including enough dilution, Big-Bang Nucleosynthesis (BBN), warm DM, hot DM, and ΔN_{eff} . Upper bounds on the DM neutrino mass and on the $SU(2)_R$ symmetry breaking scale, v_R , result from a detailed analysis of the neutrino mass matrix, which takes a form constrained by LR symmetry. Furthermore, the mass of the lightest active neutrino is constrained to be $\lesssim 10^{-4}$ eV. We discuss how the resulting parameter space will be probed observationally, especially using 21 cm cosmology, and also how it is further constrained if decays of the long-lived right-handed neutrino generate the observed baryon asymmetry via leptogenesis. The range of v_R predicted by the DM abundance is compared to ranges which lead to precision gauge coupling unification and to the observed value of the Higgs boson mass.

In addition, we study the case of lower reheating scales, finding that freeze-in is also a viable option to produce relic right-handed neutrinos. In this case, the sensitivity to the reheat temperature after inflation leads to a wide open parameter space, with values of v_R as large as the Planck scale.

2 Left-right models and neutrino masses

In this section we summarize the neutrino sector of left-right theories, emphasizing the role played by the LR symmetry. We begin by considering the effective theory of the SM with 3 additional gauge singlets, N_i , and then introduce LR symmetry. The leading operators in the SM that give rise to masses for neutrinos are bilinear in lepton fields,

$$-\mathcal{L}_{\text{SM+N,eff}} \supset y_{ij} (\ell_i N_j) H_L + \frac{y'_{ij}}{\Lambda} (\ell_i \ell_j) H_L^2 + y''_{ij} M_R (N_i N_j) + \text{h.c.} \quad (2.1)$$

where $\ell_i \equiv (\nu_i, e_i)$ are the three lepton $SU(2)_L$ -doublet fields. This involves three independent dimensionless flavor matrices (y, y', y'') and two mass scales: the SM cutoff scale Λ and the right-handed neutrino mass scale, M_R . Without N_i , the SM only contains the second of these three operators [20], which is sufficient to adequately describe the observed neutrino masses and mixings, once the SM Higgs field H_L acquires its vacuum expectation value, v . When including N_i , the second term of (2.1) is often neglected, resulting in light neutrino masses from the seesaw mechanism [21–24] if $M_R \gg v$.

In this paper we study the extension of the SM electroweak gauge group to $SU(2)_L \times SU(2)_R \times U(1)_{B-L}$. This simplifies the representation structure of the quarks and leptons: $q \equiv (u, d)$ and $\ell \equiv (\nu, e)$ transforming as (2,1) under $SU(2)_L \times SU(2)_R$ and $\bar{q} \equiv (\bar{u}, \bar{d})$ and $\bar{\ell} \equiv (N, \bar{e})$ transforming as (1,2). The presence of the right-handed neutrinos is now required by the gauge symmetry, and this is their natural setting. We impose a discrete symmetry that interchanges $SU(2)_L \leftrightarrow SU(2)_R$; the corresponding transformation on the fermions may include spacetime parity, $\ell \leftrightarrow \bar{\ell}^\dagger$, or not, $\ell \leftrightarrow \bar{\ell}$.

We do not specify the full structure of the LR symmetric theory, though any such theory must have the $SU(2)_R \times U(1)_{B-L}$ gauge symmetry broken to hypercharge at some scale $v_R \gg v$. We consider the effective field theory below v_R , assuming that the only fermions relevant for neutrino masses in the effective theory are ν_i and N_i , and the lepton-number violating contribution to their masses is generated by a single type of LR symmetric interaction. In this case, the leading operators for neutrino masses are

$$-\mathcal{L}_{\text{LR,eff}} \supset y_{ij} (\ell_i N_j) H_L + \frac{c y'_{ij}}{v_R} (\ell_i \ell_j) H_L^2 + y_{ij}^{(*)} v_R (N_i N_j) + \text{h.c.} \quad (2.2)$$

If the LR symmetry includes spacetime parity, y is a Hermitian matrix and the complex conjugation is included in the last term; otherwise y is symmetric and the complex conjugation is omitted. Even though LR symmetry has been spontaneously broken, the $(\ell_i \ell_j)$ and $(N_i N_j)$ flavor matrices are identical, $y''_{ij} = y'_{ij}$, reflecting the symmetry structure of the full theory. This will have important consequences for the parameter space in which N_1 can be DM. Furthermore, comparing with (2.1) we find that $M_R = v_R$ and $\Lambda = v_R/c$, where the constant c is discussed below, and is unity in certain theories.

The effective Lagrangian leads to a 6×6 neutrino mass matrix,

$$\begin{pmatrix} \nu_i & N_i \end{pmatrix} \begin{pmatrix} c M_{ij} v^2 / v_R^2 & y_{ij} v \\ y_{ji} v & M_{ij}^{(*)} \end{pmatrix} \begin{pmatrix} \nu_j \\ N_j \end{pmatrix}, \quad (2.3)$$

where $M_{ij} = y'_{ij} v_R$. Without loss of generality we can work in a basis where y' is diagonal such that,

$$M_{ij} = M_i \delta_{ij}, \quad (2.4)$$

with all M_i real. Upon integrating out the three heavy states, we obtain a mass matrix for the three light neutrinos:

$$m_{ij} = \delta_{ij} c \frac{v^2}{v_R^2} M_i - y_{ik} v \frac{1}{M_k} y_{jk} v \equiv \delta_{ij} m_{\nu,i}^{(5)} - m_{\nu,ij}^{(ss,N)}. \quad (2.5)$$

In this basis, in the limit that y_{ij} is diagonal the lepton flavor mixing arises entirely from the charged lepton mass matrix. Our results apply to any LR theory where neutrino physics below v_R is described by (2.2), together with the gauge interactions. Our results may not apply if there are additional states below v_R (e.g., neutral fermions with bilinear operators mixing with ν or N).

We now consider how the effective theory of (2.2) arises in two simple models. We begin with the conventional LR theory with scalar multiplets Δ_L, Δ_R and Φ which transform as (3,1), (1,3) and (2,2) under $SU(2)_L \times SU(2)_R$, respectively. This leads to the Lagrangian,

$$-\mathcal{L}_{\text{LR}} \supset y_{ij} (\ell_i \bar{\ell}_j) \Phi + y'_{ij} (\ell_i \ell_j) \Delta_L + y'^{(*)}_{ij} (\bar{\ell}_i \bar{\ell}_j) \Delta_R + \text{h.c.} . \quad (2.6)$$

With this scalar spectrum, the LR symmetry is broken by $\langle \Delta_R \rangle = v_R$, giving the $(N_i N_j)$ term of (2.2), and Φ contains the SM Higgs, H_L , giving the $(\ell_i N_j)$ term of (2.2). Finally, Δ_L acquires a mass of order v_R and, when it is integrated out of the theory, leads to the $(\ell_i \ell_j)$ term of (2.2) via the quartic interaction $\lambda_{LR} \Delta_L \Delta_R \Phi^\dagger \Phi$. The constant c is proportional to λ_{LR} , and hence c is typically of order unity or smaller; $c \gg 1$ requires fine-tuning the mass of Δ_L to be far below v_R and we do not consider this possibility.

There is a structurally simpler LR model involving just two scalar multiplets H_L and H_R transforming as (2,1) and (1,2) under $SU(2)_L \times SU(2)_R$. This theory has the virtue that, if the LR symmetry is taken to include spacetime parity, it solves the strong CP problem [10–12]. Furthermore, the vanishing of the SM Higgs quartic coupling at high energies can be understood in this theory from the Higgs Parity mechanism [12]. The pure doublet symmetry breaking leads to leptonic interactions relevant for neutrino masses above v_R of the form

$$-\mathcal{L}_{\text{LR}} \supset f_{ij} \frac{1}{\Lambda} (\ell_i \bar{\ell}_j) H_L H_R + f'_{ij} \frac{1}{\Lambda} (\ell_i \ell_j) H_L^2 + f'^{(*)}_{ij} \frac{1}{\Lambda} (\bar{\ell}_i \bar{\ell}_j) H_R^2 + \text{h.c.} , \quad (2.7)$$

where Λ is the UV cutoff for this theory. Inserting the LR symmetry breaking scale, $\langle H_R \rangle = v_R$, immediately gives (2.2), with $y_{ij}^{(l)} = f_{ij}^{(l)} v_R / \Lambda$, and the added prediction that $c = 1$.

Right-handed neutrino DM in the keV to MeV mass range requires extremely small numbers, whether in the context of (SM + N) or a LR theory. The requirement that N_1 is sufficiently light requires (in a LR theory $y'' = y'$),

$$y''_{11} \sim \begin{cases} 10^{-20} \left(\frac{M_1}{10 \text{ keV}} \right) \left(\frac{10^{15} \text{ GeV}}{M_R} \right) & (\text{SM} + N_i) \\ 10^{-15} \left(\frac{M_1}{10 \text{ keV}} \right) \left(\frac{10^{10} \text{ GeV}}{v_R} \right) & (\text{LR}) \end{cases}, \quad (2.8)$$

where we have normalized v_R to a scale intermediate between the weak and grand unification scales, which will follow from an N_1 DM production mechanism studied below. Right-handed neutrino DM runs counter to the simple seesaw understanding of why the neutrinos are much lighter than the charged fermion masses [21–24]. In (2.1), taking $\Lambda \gg 10^{15}$ GeV so that the second term is irrelevant, and taking $M_R \sim 10^{15}$ GeV, gives the observed neutrino masses for y_{ij} and y''_{ij} of order unity. Nevertheless, given the exceptionally small numbers that arise in these theories to understand the weak scale (10^{-32}) and the cosmological constant (10^{-120}), it seems worth pursuing right-handed neutrino DM, especially in LR theories where their existence is a necessity.

3 N_1 stability

We define N_1 as a cosmologically stable right-handed neutrino responsible for the DM density of the universe. Even though there is no symmetry that stabilizes N_1 , it may be sufficiently long-lived to be a DM candidate. The dominant decay of N_1 is driven by $N_1 - \nu$ mixing controlled by y_{1i} ; hence $y_{1i} \ll 1$ is needed for N_1 to be long-lived.¹

The $N_1 - \nu$ mixing angle is given by

$$\sin 2\theta_1 \equiv \frac{v}{M_1} \sqrt{\sum_i |y_{1i}|^2}, \quad (3.1)$$

where $v \simeq 174$ GeV. The experimental constraints on $\sin 2\theta_1$ arise from two different processes: For M_1 below about 3 keV, the dominant constraint on the sterile-active mixing angle comes from overproducing N_1 DM via the Dodelson-Widrow mechanism [16]. For heavier N_1 , the dominant constraint comes from overproducing photons by N_1 DM decays, most prominently through $N_1 \rightarrow \nu\gamma$ [25]:

$$\begin{aligned} \Gamma_{N_1 \rightarrow \nu\gamma} &\simeq \frac{9\alpha}{8192\pi^4} \frac{M_1^5}{v^4} \sin^2 2\theta_1, \\ &\simeq (1.5 \times 10^{30} \text{ sec})^{-1} \left(\frac{M_1}{1 \text{ keV}} \right)^5 \left(\frac{\sin^2 2\theta_1}{5 \times 10^{-9}} \right). \end{aligned} \quad (3.2)$$

As the decay rate is $\propto M_1^5$ it grows rapidly with M_1 and is a powerful constraint on the mixing angle for $M_1 \gtrsim$ keV. Sufficient stability of N_1 requires $\Gamma_{N_1 \rightarrow \nu\gamma} \lesssim 1 \times 10^{-27} \text{ s}^{-1}$ [25] and hence

$$|y_{1i}| \lesssim 10^{-13} \left(\frac{10 \text{ keV}}{M_1} \right)^{3/2} \quad (M_1 \gtrsim 3 \text{ keV}). \quad (3.3)$$

The combination of the constraints leads to a limit on the mixing angle [25],

$$\sin^2 2\theta_1 \leq 5 \times 10^{-9} \begin{cases} \left(\frac{M_1}{3 \text{ keV}} \right)^{-1.8} \times D & \text{(Overproduction)} \\ \left(\frac{M_1}{3 \text{ keV}} \right)^{-5} & \text{(Decay)}. \end{cases} \quad (3.4)$$

¹Note that our numbering of SM neutrinos does not necessarily coincide with the neutrino numbering commonly found in the literature.

D is the dilution factor required to reduce a thermal yield of N_1 to the correct DM abundance. The higher photometric sensitivities of next generation x-ray and gamma-ray telescopes such as ATHENA [26] and e-ASTROGAM [27] may probe an order of magnitude smaller $\sin^2 2\theta_1$ [28]. For $M_1 > 1$ MeV, the tree-level decay $N_1 \rightarrow e^+e^-\nu$ is open and the resultant constraint on y_{1i} is similar to (3.3).

The smallness of the Yukawa coupling in (3.3) can be explained in the SM+ N_i theory by imposing a discrete Z_2 symmetry under which N_i are odd so that the last operator of (2.1) is forbidden, giving $y_{1i} = 0$ and making N_1 stable. Furthermore, introducing an inert doublet H'_L , that has no vacuum expectation value and is odd under this parity, allows the first operator of (2.1) to be generated from a 1-loop radiative correction [29]. In the LR framework, a Z_2 symmetry that sets $y_{1i} = 0$ also forbids charged lepton Yukawa couplings. However, in a LR theory one can alternatively impose a discrete $Z_{4L} \times Z_{4R}$ symmetry setting $y_{1i} = 0$, guaranteeing cosmologically stable N_1 , while allowing charged lepton masses. We discuss how the model works in Appendix B.

If kinematically allowed, N_1 can also beta decay via W_R exchange to $\ell^\pm + \text{hadron(s)}$, where ℓ^\pm is any charged lepton, regardless of how small y_{1i} is. The inclusive decay rate is,

$$\begin{aligned} \Gamma_{N_1 \rightarrow \ell^\pm + \text{hadrons}} &\simeq \frac{3}{1536\pi^3} \frac{M_1^5}{v_R^4} \\ &\simeq (1.4 \times 10^{24} \text{ sec})^{-1} \left(\frac{M_1}{150 \text{ MeV}} \right)^5 \left(\frac{v_R}{10^{10} \text{ GeV}} \right)^{-4}. \end{aligned} \quad (3.5)$$

For sufficiently small M_1 or large v_R , this is below the observational upper bounds of $\sim 10^{25}$ sec [30].² Here the decay rate is estimated in the quark picture, but the interpolation to the meson regime $M_1 \gtrsim m_\pi$ is correct at the order of magnitude level.

For M_1 below the pion mass, beta decay to $\ell^+\ell^-\nu$ via $W_R - W_L$ mixing is important. This decay channel is also independent of y_{1i} and given by

$$\Gamma_{N_1 \rightarrow \ell^+\ell^-\nu} \simeq \frac{\Gamma_{N_1 \rightarrow \ell^\pm + \text{hadrons}}}{3} \times \begin{cases} 1 & : (2,2) \text{ Breaking} \\ \left(\frac{1}{16\pi^2} \frac{m_b m_t}{v^2} \ln \left(\frac{\Lambda}{v} \right) \right)^2 & : (2,1)+(1,2) \text{ Breaking.} \end{cases} \quad (3.6)$$

When the electroweak symmetry is broken by an $SU(2)_L \times SU(2)_R$ bi-fundamental scalar, its vacuum expectation value gives a $W_R - W_L$ mixing at tree-level. If the electroweak symmetry is broken by an $SU(2)_L$ doublet scalar, the mixing is generated by a top/bottom quark loop. The quantum correction is logarithmically divergent in the effective theory where the quark masses are given by dimension-5 operators, similar to Eq. (2.7). The scale Λ that cuts off the divergence is model-dependent, but is close to v_R since the top and bottom Yukawa couplings are not small.

²Although N_1 decays via W_R to charged pions which then decay to muons, for $M_1 \gg m_\pi$, there may be a large number of neutral pions in the decay shower, which subsequently decay to hard photons and yield slightly stronger constraints on the N_1 lifetime [30].

The $W_R - W_L$ mixing also induces the decay of N_1 into $\nu\gamma$ [19, 31, 32]. Connecting the $\ell^+\ell^-$ in the beta-decay diagram and attaching an external photon to this loop gives a decay rate

$$\Gamma_{N_1 \rightarrow \nu\gamma} \simeq \frac{\alpha}{4\pi} \frac{m_\tau^2}{M_1^2} \Gamma_{N_1 \rightarrow \ell^+\ell^-\nu}, \quad (3.7)$$

which is observationally limited by photon searches to be less than about $10^{-27} s^{-1}$.

4 Relativistic freeze-out and dilution

The right-handed neutrinos couple to the SM bath via W_R exchange. If the reheat temperature of the universe after inflation is sufficiently high,

$$T_{\text{RH}}^{\text{inf}} \gtrsim 10^8 \text{ GeV} \left(\frac{v_R}{10^{10} \text{ GeV}} \right)^{4/3}, \quad (4.1)$$

the right-handed neutrinos reach thermal equilibrium and subsequently decouple with a thermal yield $Y_{\text{th}} \simeq 0.004$.³ For N_1 to have the observed DM abundance requires $m_{N_1} \simeq 100$ eV; however, such light sterile neutrino DM is excluded by the Tremaine-Gunn [33–35] and warmness [36–39] bounds; see [25] for a recent review.

Nevertheless, it is still possible to realize N_1 as DM with $M_1 \gtrsim \text{keV}$, if they decouple relativistically from the thermal bath and their abundance is diluted. If another right-handed neutrino, N_2 , is sufficiently long-lived such that it comes to dominate the energy density of the universe and produces entropy when it decays, it can dilute the DM abundance and cool N_1 below warmness bounds [19, 40]. The relic density of N_1 is

$$\begin{aligned} \frac{\rho_{N_1}}{s} &= 1.6 \frac{3}{4} \frac{M_1}{M_2} T_{\text{RH}}, \\ \Rightarrow \frac{\Omega_{N_1}}{\Omega_{\text{DM}}} &\simeq \left(\frac{M_1}{10 \text{ keV}} \right) \left(\frac{300 \text{ GeV}}{M_2} \right) \left(\frac{T_{\text{RH}}}{10 \text{ MeV}} \right), \end{aligned} \quad (4.2)$$

where the numerical factor 1.6 is taken from [41], ρ_{N_1} is the energy density, s is the entropy density, $\Omega_{\text{DM}} \simeq 0.25$ is the observed cosmic relic abundance, and T_{RH} is the decay temperature of N_2 , as set by its total decay rate Γ_{N_2}

$$T_{\text{RH}} = \left(\frac{10}{\pi^2 g_*} \right)^{1/4} \sqrt{\Gamma_{N_2} M_{\text{Pl}}}. \quad (4.3)$$

These formulae are also applicable to the case where N_3 first dominates the universe and decays to create entropy, and later N_2 dominates and creates entropy again. Inserting the

³The analysis in this section is also applicable to lower $T_{\text{RH}}^{\text{inf}}$ as long as N_1 and N_2 are frozen-in from W_R exchange, and N_1 is overproduced as DM (see Eq. (7.2)). In such a scenario, the required dilution to realize N_1 DM is diminished, and hence the warmness constraints on N_1 slightly increase above 2 keV. See Fig. 4 for the warmness constraints on a pure freeze-in cosmology without any dilution.

warmness bound on N_1 , ($M_1 > 2 \text{ keV}$, see Sec. 5.1), and the reheating bound from hadronic decays of N_2 during BBN ($T_{\text{RH}} > 4 \text{ MeV}$) [42–44],⁴ into (4.2) requires⁵

$$M_2 \gtrsim 24 \text{ GeV}. \quad (\text{Warmness, reheating, DM abundance}). \quad (4.4)$$

There are several possible decay modes for N_2 , and which one dominates varies with M_2 . N_2 can always beta decay through W_R exchange into right-handed fermions, $N_2 \rightarrow (\ell^+ \bar{u} d, \ell^- u \bar{d})$ and $N_2 \rightarrow N_1 \ell^+ \ell^-$. These decay channels are unavoidable as they are independent of the free-parameter y_{2i} , and prevent N_2 from efficiently diluting N_1 in some regions of parameter space. The N_2 decay rate via W_R exchange is

$$\Gamma_{N_2 \rightarrow N_1 \ell^+ \ell^-} + \Gamma_{N_2 \rightarrow (\ell^+ \bar{u} d, \ell^- u \bar{d})} = \frac{1}{1536\pi^3} \frac{M_2^5}{v_R^4} \times 20. \quad (4.5)$$

In addition, when $M_2 \gtrsim v$, N_2 can decay at tree-level via $N_2 \rightarrow \nu h, \nu Z, \ell^\pm W^\mp$ while for $M_2 \lesssim v$, N_2 can beta decay through W_L/Z exchange and active-sterile mixing to SM fermions, $N_2 \rightarrow \ell u d, \ell^+ \ell^- \nu, \nu \nu \bar{\nu}$. These decay rates are given by

$$\Gamma_{N_2 \rightarrow \ell H_L} = \frac{1}{8\pi} \sum_i |y_{2i}|^2 M_2 \quad (M_2 \gtrsim v) \quad (4.6)$$

$$\Gamma_{N_2 \rightarrow (\ell^+ \bar{u} d, \ell^+ \ell^- \bar{\nu}, \nu \nu \bar{\nu} \text{ or h.c.})} \simeq \frac{171}{8} \frac{1}{1536\pi^3} \frac{M_2^3}{v^2} \sum_i |y_{2i}|^2 \quad (M_2 \lesssim v). \quad (4.7)$$

For the latter we add up the results in [19, 48] in the limit of a vanishing Weinberg angle, for simplicity. In either case, y_{2i} must be sufficiently small so that N_2 dominates the energy density of the universe before decaying. Diluting N_1 to the observed DM abundance requires

$$|y_{2i}| \lesssim \begin{cases} 3 \times 10^{-10} \left(\frac{M_2}{24 \text{ GeV}} \right)^{-1/2} \left(\frac{M_1}{2 \text{ keV}} \right)^{-1} & (M_2 \lesssim v) \\ 1 \times 10^{-11} \left(\frac{M_2}{v} \right)^{1/2} \left(\frac{M_1}{2 \text{ keV}} \right)^{-1} & (M_2 \gtrsim v). \end{cases} \quad (4.8)$$

The equality sign applies when the contribution to the N_2 decay rate from W_R exchange, (4.5), is sub-dominant.

⁴Low reheating temperatures can also affect the CMB since some decays occur after neutrinos decouple, reducing the effective number of neutrinos [42, 43, 45]. In our case, N_2 also decays into neutrinos and the bound from the CMB, $T_{\text{RH}} > 4 \text{ MeV}$ [46], may be relaxed.

⁵Ref. [47] points out that if the mass eigenstate N_1 forms an $SU(2)_R$ doublet with the mass eigenstate τ , it might be possible for N_1 to decouple earlier than N_2 because of the Boltzmann-suppressed density of τ relative to μ or e . This reduces the relic density of N_1 compared to N_2 which relaxes the necessary dilution from N_2 by a factor of 3–4 and hence lowers the bound on M_2 from 24 GeV to 6–8 GeV. However, if N_2 decouples after N_1 , its density is Boltzmann-suppressed since $M_2 \gg m_\tau$, making dilution ineffective. Consequently, we find that the potential relaxation of the bound on M_2 (4.4) unattainable. Ref. [47] also points out that if N_2 forms an $SU(2)_R$ doublet with μ and $M_2 \simeq m_\mu + m_\tau \simeq 250 \text{ MeV}$, the decay rate of N_2 via W_R exchange is suppressed by a small phase space, allowing N_2 to be long-lived and provide sufficient dilution even for v_R around the TeV scale. Since we find that the possible relaxation of the lower bound on M_2 does not work, we also cannot confirm this claim.

In Appendix A, we use the above results, together with the radiative stability bound on N_1 , to derive constraints on the neutrino mass matrix of (2.5).

1. For $M_1 < M_3$, we show that the lightest neutrino mass eigenstate is closely aligned with ν_1 and has a mass $m_1 \ll \sqrt{\Delta m_{\text{sol}}^2}$. In the case that $M_3 > M_2$, the other two mass eigenstates are very close to ν_2 and ν_3 and have masses $m_2 = c(v^2/v_R^2)M_2$ and $m_3 = c(v^2/v_R^2)M_3 - y_{33}^2 v^2/M_3$. For $M_3 < M_2$, the (2,3) entry of the mass matrix may be non-negligible, so that the two heavy active mass eigenstates are each linear combinations of $\nu_{2,3}$. In this case, we are able to derive a relation between the scale of their masses and M_2 : $M_2 \simeq \mu(v_R/v)^2 c^{-1}$, where $0.01 \text{ eV} \lesssim \mu \lesssim 0.10 \text{ eV}$. In the rest of the paper we take

$$M_2 \simeq m_2 \left(\frac{v_R}{v} \right)^2 \frac{1}{c}, \quad (4.9)$$

but, in the case that $M_3 < M_2$, m_2 should be taken in the range (0.01 – 0.10) eV and not set to an active neutrino mass eigenvalue.

2. For $M_1 > M_3$, we show that the lightest neutrino mass is much smaller than $\sqrt{\Delta m_{\text{sol}}^2}$ and that M_2 is given by Eq. (4.9), with the parameter c replaced by a parameter $c_{\text{eff}} < c$.

In Fig. 1, we show the constraints on (v_R, M_1) when $m_2 = \sqrt{\Delta m_{\text{atm}}^2}$ (**left**) and $m_2 = \sqrt{\Delta m_{\text{sol}}^2}$ (**right**). In the orange shaded region, the required T_{RH} is below 4 MeV, which is excluded by hadronic decays of N_2 during BBN [42, 43]. The green-shaded region is excluded due to the warmth of N_1 affecting large scale structure. To the right of the blue line, the beta decay rate of N_2 via W_R exchange is the dominant contribution to Γ_{N_2} ; here, the dilution of N_1 is chiefly through $N_2 \rightarrow N_1 \ell^+ \ell^-$ and $N_2 \rightarrow (\ell^+ \bar{u} d, \ell^- u \bar{d})$. Using (4.9), these decay rates scale as a positive power of M_2 and hence v_R . Within the blue-shaded region, the N_2 decay rate becomes too fast to efficiently dilute the N_1 energy density.

The blue line itself is an interesting region of parameter space, which does not require any tuning but simply corresponds to the limit where the dominant decay is set entirely by the W_R exchange terms in (4.5). In this limit the N_1 abundance has two contributions: from N_2 decay through $N_2 \rightarrow N_1 \ell^+ \ell^-$ as well as the abundance from relativistic decoupling. While the latter is the dominant component, the former can also make up a significant component of DM, which can be probed by future experiments as discussed in Sec. 5.2.

As can be seen from Fig. 1, the allowed region of frozen-out N_1 DM from LR theories forms a bounded triangle in the $v_R - M_1$ plane. The position and size of the triangle depends on c , such that the allowed region shrinks in size and shifts to lower v_R for smaller c . This is because the $\Omega_{N_1} > \Omega_{\text{DM}}$ bound depends more sensitively on M_2 (and hence c) than the $T_{\text{RH}} < 4 \text{ MeV}$ bound. We show the effect of c on the allowed region for three values of c : one near the experimental minimum, one near the natural maximum, and one in between. As can be seen by the smallest triangle of Fig. 1, the allowed region of N_1 DM disappears for $c \lesssim 1 \times 10^{-4}$, placing an experimental lower bound on $v_R \gtrsim 10^6 \text{ GeV}$. Similarly, the naturalness argument

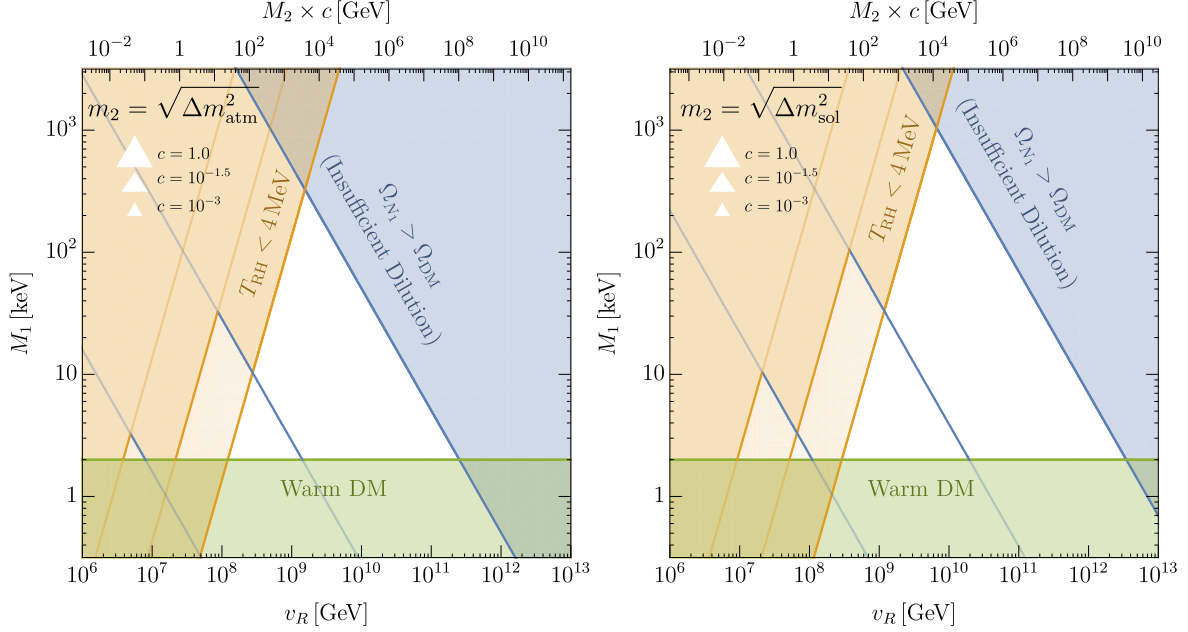


Figure 1. The parameter space of N_1 DM produced by relativistic freeze-out and dilution from N_2 decay: constraints on the LR symmetry breaking scale v_R and the mass N_1 . The constraints from warm DM are in **green**, Big Bang Nucleosynthesis in **orange**, and insufficient dilution in **blue**. The constraints depend on the LR-model dependent parameter $c \lesssim 1$. **Left:** We fix the ν_2 mass by the atmospheric neutrino mass difference, $m_2 = \sqrt{\Delta m_{\text{atm}}^2}$. **Right:** We fix the ν_2 mass by the solar neutrino mass difference, $m_2 = \sqrt{\Delta m_{\text{sol}}^2}$.

discussed in Sec. 2 limits c near unity, and an upper bound on $v_R \lesssim 10^{13}$ GeV as shown by the largest triangle of Fig. 1. For the remainder of this paper, we conservatively focus on the case $c = 1$, the largest naturally allowed parameter space of N_1 DM, when considering signals and future experimental probes.

5 Signals and future probes

So far we have focused on the current constraints on sterile neutrino DM in general LR theories and found freeze-out to be a viable option as long as the c parameter, characterizing the seesaw contribution to the light neutrino masses, is not too small. In this section, we discuss how future observations can probe the parameter space through dark radiation, warm DM, and additional structure on very small scales. In addition, the requirement of viability of leptogenesis greatly restricts the parameter space.

5.1 Warmness

The free-streaming length of thermally produced N_1 can be large if N_1 is light. When M_1 is $\mathcal{O}(\text{keV})$, the free-streaming length of N_1 approaches the size of galactic mass perturbations, suppressing the matter power spectrum on scales $k \gtrsim 0.1 \text{ Mpc}^{-1}$ [49–53]. A suppression can

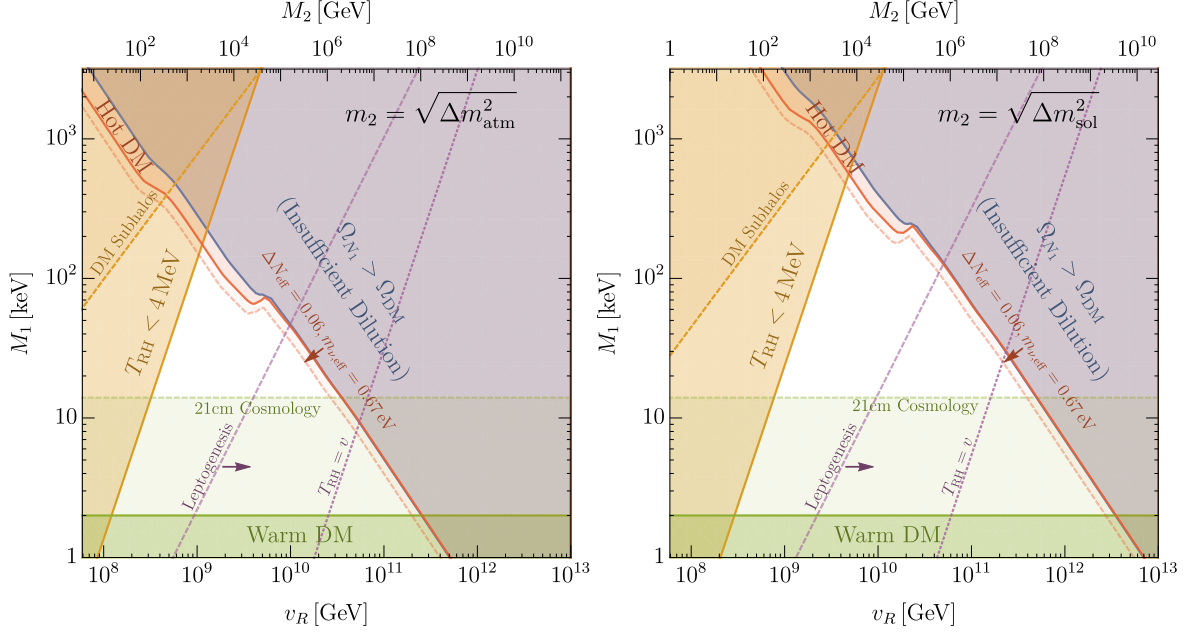


Figure 2. The parameter space of N_1 DM produced by relativistic freeze-out and dilution from N_2 decay in terms of the left-right symmetry breaking scale, v_R , and the mass of N_1 , M_1 , for $c = 1$. We show constraints from N_2 decaying after Big Bang Nucleosynthesis (orange), decaying too early to provide sufficient N_1 dilution (blue), warm DM bounds (green), and hot DM bounds (red). In addition we show prospects of future surveys of T_{RH} from pulsar timing on DM subhalos (dashed orange), improved searches for hot DM from CMB telescopes (dashed red), and warm DM from 21-cm cosmology (dashed green). Lastly, to the left of the dashed purple curve labeled ‘Leptogenesis’, the baryon asymmetry produced by N_2 decays is insufficient due to dilution and sphalerons, even with $\epsilon = 1$. **Left:** We fix the ν_2 mass with the atmospheric neutrino mass difference, $m_2 = \sqrt{\Delta m_{\text{atm}}^2}$. **Right:** We fix the ν_2 mass with the solar neutrino mass difference, $m_2 = \sqrt{\Delta m_{\text{sol}}^2}$.

be observed through large scale structure surveys, perturbations in the cosmic microwave background (CMB), or absorption of low-redshift Lyman- α photons by neutral hydrogen (a tracer of DM) in the intergalactic medium [54–57]. For N_1 that was thermally produced and diluted to the observed DM abundance, the bounds are at $\mathcal{O}(1 - 5 \text{ keV})$ range. We adopt $M_1 \gtrsim 2 \text{ keV}$ as our constraint in the dark green region of Fig. 2. Future 21-cm cosmology experiments, which can trace early star and galaxy formation at cosmic dawn, are anticipated to probe the matter power spectrum on scales $k \gtrsim 50 \text{ Mpc}^{-1}$. If no suppression on such scales is observed, searches would constrain $M_1 \gtrsim 14 \text{ keV}$ [58], which we show with the dashed green region of Fig. 2.

5.2 Hotness

Although N_1 DM is dominantly produced thermally, a subdominant fraction is always produced non-thermally (see section 4). Specifically, the beta decay $N_2 \rightarrow N_1 \ell^+ \ell^-$ produces relativistic N_1 . This non-thermal population of N_1 becomes non-relativistic at temperatures

$\mathcal{O}(\text{eV})$ and contributes a hot component of DM. Constraints on hot DM are conventionally given in terms of the effective number of neutrino species, ΔN_{eff} , which parameterizes its energy density while relativistic, and the effective neutrino mass, $m_{\nu,\text{eff}}$, which parameterizes its energy density when it has become non-relativistic matter [56, 59]. For LR models, this is given by

$$\Delta N_{\text{eff}} = \frac{1}{3} \text{Br}(N_2 \rightarrow N_1 \ell^+ \ell^-) \left(\frac{g_{*,\text{eq}}^4}{g_{*,T_{\text{RH}}}} \right)^{\frac{1}{3}} \frac{4}{7} \left(\frac{4}{11} \right)^{-\frac{4}{3}} \simeq 0.97 \text{Br}(N_2 \rightarrow N_1 \ell^+ \ell^-) \left(\frac{106.75}{g_{*,T_{\text{RH}}}} \right)^{\frac{1}{3}},$$

$$m_{\nu,\text{eff}} \equiv 94.1 \text{ eV } \Omega_{N_1,\text{hot}} h^2 \simeq 11 \text{ eV } \text{Br}(N_2 \rightarrow N_1 \ell^+ \ell^-). \quad (5.1)$$

When the W_R -exchange decay is subdominant, $\text{Br}(N_2 \rightarrow N_1 \ell^+ \ell^-)$ scales as $M_1^2 v_R^2$, and it saturates at 0.1 (since 90% of beta decays produce quarks and no N_1) along the blue curve. Along this line a significant amount of hot DM is predicted: $\Delta N_{\text{eff}} \simeq 0.1$ and $m_{\nu,\text{eff}} \simeq 1.1 \text{ eV}$. Coincidentally, current limits on the two-dimensional marginalized distribution of ΔN_{eff} and $m_{\nu,\text{eff}}$ already require $\Delta N_{\text{eff}} \lesssim 0.1$ and $m_{\nu,\text{eff}} \lesssim 1.0 \text{ eV}$ [59], which we indicate by the red-shaded region labeled ‘Hot DM’ in Fig. 2.

CMB Stage IV [60], a collection of future ground based telescopes, will be able to search for hot DM signals inside the currently allowed region. Assuming a null detection, the experiment will be able limit $\Delta N_{\text{eff}} \lesssim 0.06$ [61], which we show by the dashed red region of Fig. 2.⁶ Note that for $v_R \lesssim 10^{10} \text{ GeV}$, T_{RH} occurs below the QCD phase transition, which is accompanied by a sharp decrease of $g_{*,T_{\text{RH}}}$, leading to an enhancement in ΔN_{eff} and strengthening the red-shaded region. The limit where the the dominant decay of N_2 is set by the W_R exchange can be probed by CMB Stage IV.

5.3 Early matter dominated era

The current bound on the reheat temperature, $T_{\text{RH}} \gtrsim 4 \text{ MeV}$, comes from N_2 decaying during BBN, leading to its decay products altering the neutron to proton ratio enough to conflict with the observed light element abundances [42, 43]. Presently, ideas to probe higher reheat temperatures rely on the cosmological effects of the early matter dominated era, namely the formation of ultra compact DM halos [64, 65]. For example, halos with masses as low as $M_{\text{halo}} \simeq 10^{-10} M_{\odot}$ can be observed with pulsar timing arrays once the Square Kilometer Area [66] is built [67] (in principle, gravitational microlensing could also be used to look for sub-halos from early matter domination, but such halos would typically have concentration parameters of $\mathcal{O}(10^3)$ and would be too diffuse to have a sizable signature [67–69]). The largest DM halo masses are correlated with T_{RH} since the density perturbations, $k(a) \equiv aH(a)$, which enter the horizon during the early matter dominated era and source the halos, are largest just before reheating:

$$M_{\text{halo}} \approx \frac{4}{3} \pi k_{\text{RH}}^{-3} \rho_{m,0} \approx 10^{-10} M_{\odot} \left(\frac{T_2}{500 \text{ MeV}} \right)^{-3} \left(\frac{g_{*s}(T_2)}{68} \right) \left(\frac{g_*(T_2)}{68} \right)^{-3/2}. \quad (5.2)$$

⁶Future space based telescopes such as CORE can theoretically detect $m_{\nu,\text{eff}} \sim 0.04 \text{ eV}$ at 1σ , but only if $\Delta N_{\text{eff}} \gtrsim 0.05$ [62, 63].

Here, $k_{\text{RH}} = a(T_{\text{RH}})H(T_{\text{RH}})$ is the scale of density perturbations entering the horizon at T_{RH} , and $\rho_{m,0}$ is the present-day mass density of non-relativistic matter [64]. From (5.2), we see that pulsar timing arrays can probe reheat temperatures as high as ~ 500 MeV.

An important caveat to these experimental searches arises when DM has such a large free-streaming length that ultra compact halos cannot form during the early matter-dominated era. The free-streaming length of N_1 DM is [70]

$$\lambda_{\text{FS}} \equiv \int_0^{t_{\text{eq}}} \frac{v(a)}{a} dt \leq \int_{t_{\text{RH}}}^{t_{\text{eq}}} \frac{v(a)}{a} dt = \frac{1}{H_{\text{RH}} a_{\text{RH}}^2} \frac{\langle p_{\text{dec}} \rangle a_{\text{dec}}}{M_1} \ln \left(\frac{h(a_{\text{eq}})}{h(a_{\text{RH}})} \right), \quad (5.3)$$

where $h(a) \equiv \sqrt{a^2 + (\langle p_{\text{dec}} \rangle a_{\text{dec}} / M_1)^2} + a$ and,

$$\langle p_{\text{dec}} \rangle \simeq 3.2 T_{\text{eq}} \frac{a_{\text{eq}}}{a_{\text{dec}}} \left(\frac{g_{*s,\text{eq}}}{g_{*s,\text{dec}}} \frac{\rho_{\text{DM}}/s}{M_1 Y_{\text{therm}}} \right)^{1/3} \quad (5.4)$$

is the average momentum of N_1 upon decoupling from the SM bath. When $\lambda_{\text{FS}} \gtrsim k_{\text{RH}}^{-1}$, gravitational lensing and pulsar timing array searches cannot put a bound on T_{RH} since ultra compact halo objects do not exist in the present universe [64], as shown by the dashed orange line of Fig. 2. From this bound, we see that probing reheat temperatures above 4 MeV through observations of ultra compact DM halos requires $M_1 \gtrsim \text{MeV}$, which is already excluded by the insufficient dilution of N_1 DM.

5.4 Leptogenesis

Besides providing an excellent DM candidate in the form of N_1 , right-handed neutrinos are also appealing in that they can generate the observed baryon asymmetry via leptogenesis [71]. In a forthcoming paper [72], we show that the decay of a heavier, long-lived right-handed neutrino, N_2 , can not only provide the dilution necessary to realize N_1 DM, but also generate a large lepton asymmetry. In the usual way, this lepton asymmetry is converted to a baryon asymmetry via electroweak sphalerons, generating the observed baryon asymmetry of our universe. Since the sphaleron process ceases operation at temperatures below the weak scale, baryogenesis is suppressed when $T_{\text{RH}} < v$. In this case, the baryon asymmetry is generated by the fraction $(T_{\text{RH}}/v)^2$ of N_2 that decay in the N_2 MD-era before the temperature of the universe falls below the weak scale.⁷ Consequently, the generated baryon asymmetry is

$$Y_B = \frac{28}{79} \times \epsilon \frac{3 T_{\text{RH}}}{4 M_2} \left(\frac{T_{\text{RH}}}{v} \right)^2 \quad (5.5)$$

where ϵ is the lepton asymmetry generated per N_2 decay, and the factor of 28/79 accounts for the conversion of the lepton asymmetry into the baryon asymmetry via sphalerons [74].

⁷When $v \simeq T_{\text{RH}}$, the thermal bath is not primordial but generated by N_2 itself (see e.g. [70, 73]), and the suppression is $(T_{\text{RH}}/v)^4$.

Independent of the model, ϵ is at most unity.⁸ Conservatively taking this maximum ϵ , we see from Eq. (5.5) that generating the observed baryon asymmetry, $Y_B \simeq 8 \times 10^{-11}$, is impossible when $T_{\text{RH}} \ll v$, as shown by the dashed purple contour of Fig. 2. This constraint demonstrates that incorporating leptogenesis into N_1 DM from LR models severely diminishes the viable parameter space, and that future 21-cm cosmological probes of warm DM can significantly probe this reduced parameter space.

6 Predictions on v_R from UV physics

The cosmologically allowed region of initially thermalized N_1 DM in LR theories constrains the $SU(2)_R$ symmetry breaking scale v_R well above the electroweak scale. As discussed in Sec. 4, the viable region of the right-handed breaking scale is $10^6 \lesssim v_R/\text{GeV} \lesssim 10^{13}$, for any $c \leq 1$, and $10^8 \lesssim v_R/\text{GeV} \lesssim 10^{13}$ for the case of $c = 1$. In this section, we consider the implications such a breaking scale has on prospective theories behind LR models.

6.1 Small Higgs quartic coupling at high energy scales

Intriguingly, this range of v_R is predicted independently within ‘Higgs-Parity’ theories [12–15], a subset of LR models with Higgs-doublets H_L and H_R and with the LR symmetry spontaneously broken by $\langle H_R \rangle \gg \langle H_L \rangle$. In Higgs-Parity models, the SM Higgs quartic coupling λ is predicted to vanish at the scale v_R . The SM renormalization group flow of λ shows that $\lambda = 0$ for $10^9 \lesssim v_R/\text{GeV} \lesssim 10^{13}$, with an uncertainty dominantly arising from an uncertainty in the top quark mass [75].

This is shown explicitly in Fig. 3. The green band shows the relation between v_R and the top quark mass, m_{top} .⁹ The width of this green band arises from the uncertainty of the Higgs mass $m_h = 125.18 \pm 0.16$ GeV and the strong coupling constant $\alpha_s(m_Z) = 0.1181 \pm 0.0011$ at 2σ [76]. The preferred value of the top quark mass (2σ) is shown by a horizontal gray band. As a result, the LR symmetry breaking scale v_R is predicted to be $10^9 \lesssim v_R/\text{GeV} \lesssim 10^{13}$. The narrower green band shows the relation assuming that the uncertainties shrink to $m_h = 125.18 \pm .020$ GeV and $\alpha_s(m_Z) = 0.1181 \pm 0.0001$, which is possible through improved lattice calculations, measurements at future lepton colliders, and measurements at HL-LHC [77–79]. The top quark mass can be measured with an accuracy of a few tens of MeV by e^+e^- colliders [80–83] such as ILC [84], narrowing down the prediction on v_R within a few tens of percent, as shown by the narrower gray band. In future work, we will incorporate leptogenesis from N_2 decays with N_1 DM within the Higgs Parity framework [72].

⁸Large ϵ requires a large Yukawa coupling y_{33} , which naively produces too large SM neutrino masses by the see-saw from N_3 . This can be avoided by a certain structure in y_{ij} and y_{ij} . The magnitude of ϵ is also restricted by the stability of N_1 against quantum correction from y_{33} , further constraining the parameter space. We study this in detail in a future work.

⁹We ignore a UV completion-dependent part of the threshold correction to $\lambda(v_R)$ from m_{top} that in some extreme cases can lower the value of v_R by 1 – 2 orders of magnitude [14].

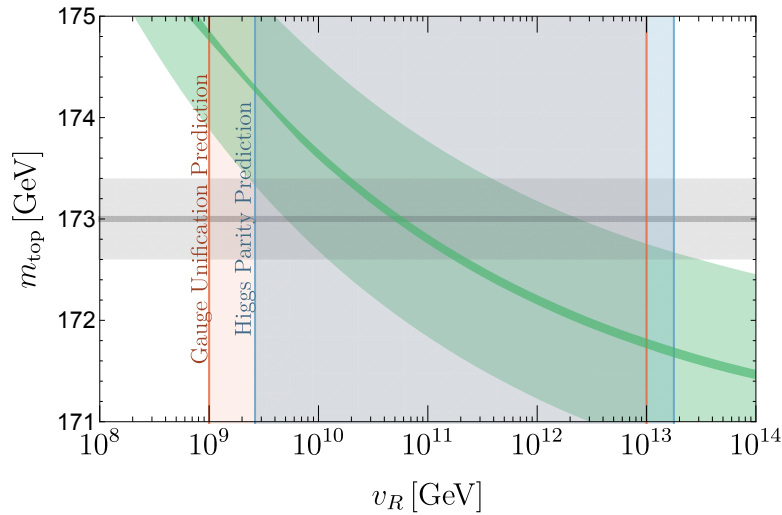


Figure 3. The predicted top quark mass in Higgs Parity theories is shown in **green**, as a function of the right-handed symmetry breaking scale. The experimentally preferred top mass is shown as a **gray** band, leading to the preferred range of v_R shown by the vertical **blue** band. The **red** band shows the range of v_R preferred by gauge coupling unification.

6.2 Gauge coupling unification

The cosmologically allowed range of v_R is also consistent with gauge coupling unification. The LR symmetric gauge group, $SU(3)_c \times SU(2)_L \times SU(2)_R \times U(1)_{B-L}$ is a subgroup of an $SO(10)$ unified gauge group. Assuming the minimal symmetry breaking chain containing the LR symmetric gauge group as an intermediate scale gauge group,

$$SO(10) \longrightarrow SU(3)_c \times SU(2)_L \times SU(2)_R \times U(1)_{B-L} \xrightarrow{v_R} SU(3)_c \times SU(2)_L \times U(1)_Y, \quad (6.1)$$

the scale v_R is predicted to be $10^9 \lesssim v_R/\text{GeV} \lesssim 10^{13}$ [14, 85, 86].

We note, however, that a stable right-handed neutrino, N_1 , is in tension with matter unification. In fact, if the SM quarks and leptons as well as the right-handed neutrinos are unified into a **16** representation of $SO(10)$, Yukawa unification naively predicts that the right-handed neutrinos are all heavy and unstable. To evade this naive expectation would require a more sophisticated model in a four-dimensional $SO(10)$ unified theory. This could be possible with $SO(10)$ unification in higher dimensions with orbifolding [87–90], where Yukawa couplings do not necessarily unify if matter is localized on gauge symmetry breaking branes [91]. Even if matter lives in the bulk, the SM quarks and leptons as well as the right-handed neutrinos may arise from zero-modes of different **16**s by the orbifold projections, as is realized in $SU(5)$ [90, 91] or $SO(10)$ [92] unification without intermediate gauge symmetry. Breaking of $SO(10)$ down into LR symmetry by orbifolding is discussed in [93].

7 Freeze-In

When the reheat temperature of the universe is below the thermalization temperature of the right-handed neutrinos (see (4.1)), neither N_1 nor N_2 have a thermal abundance. Instead, the N_1 abundance is determined by scattering via heavy W_R and Z_R exchange which, being UV-dominated, depends on the reheating temperature,

$$\frac{\rho_{N_1}}{s} \simeq 1 \times 10^{-5} \frac{M_1 (T_{\text{RH}}^{\text{inf}})^3 M_{\text{Pl}}}{v_R^4}, \quad (7.1)$$

$$\Rightarrow \frac{\Omega}{\Omega_{\text{DM}}} \simeq \left(\frac{M_1}{150 \text{ keV}} \right) \left(\frac{10^{10} \text{ GeV}}{v_R} \right)^4 \left(\frac{T_{\text{RH}}^{\text{inf}}}{10^7 \text{ GeV}} \right)^3. \quad (7.2)$$

Freeze-in production from other sources, such as $\ell H \rightarrow N_1$, are subdominant since $y_{1i} \ll 1$ is needed to ensure N_1 is long-lived. Contributions to the N_1 abundance may also arise from beta decays of N_2 and N_3 . These, however, are always subdominant to the direct freeze-in production of N_1 , whether $N_{2,3}$ are produced by the W_R interaction or the ℓNH interaction.

In Fig. 4, we show the contours of the required reheat temperature after inflation to freeze-in N_1 DM for a given (v_R, M_1) . In the green region, the warmth of N_1 affects large scale structure. Since frozen-in N_1 is never diluted, it is warmer than frozen-out N_1 for a fixed M_1 . More concretely, its free-streaming length is larger by a factor of approximately $\frac{4}{3.2} \left(\frac{M_1 Y_{\text{therm}}}{\rho_{\text{DM}}/s} \right)^{1/3}$, which gives a commensurately stronger warm DM bound compared to Fig. 2. Here, the factor of 4/3.2 comes from the difference in $\langle p/T \rangle$ for the non-thermal frozen-in distribution, to the thermal frozen-out distribution, as discussed in [94]. In the blue and pink regions, the decay of N_1 mediated by W_R , (3.5), or $W_R - W_L$ mixing, (3.7), overproduces the observed amount of galactic gamma-rays, respectively [30]. Similarly, the decay of N_1 via active-sterile mixing overproduces the observed galactic x-rays and gamma-rays for the mixing angle $\sin^2 2\theta_1$ labeling the purple dotted contours. Unlike the W_R -mediated decay, which is fixed by v_R , the decay via $N_1 - \nu$ mixing is set by the free parameter θ_1 . Lastly, searches at the LHC for heavy charged boson resonances ($pp \rightarrow W_R \rightarrow N_1 \ell$) [95] and neutral boson resonances ($pp \rightarrow Z_R \rightarrow \ell^+ \ell^-$) [96] exclude v_R below about 10 TeV, as shown by the orange region.

Fig. 4 shows that the parameter space for N_1 DM from freeze-in is weakly constrained compared to that of N_1 DM from freeze-out and dilution, shown in Fig. 1. For example, v_R could be as low as about 100 TeV, with the reheat temperature after inflation below 100 GeV. Likewise, bounds on M_1 are weak; although as M_1 increases $\sin^2 2\theta_1$ is constrained to become extremely small to keep N_1 sufficiently long-lived. However, if leptogenesis via N_2 decay is incorporated into the N_1 DM freeze-in cosmology, the (M_1, v_R) parameter space becomes more tightly constrained. In a future work, we discuss this viable parameter space in the framework of Higgs Parity [72].

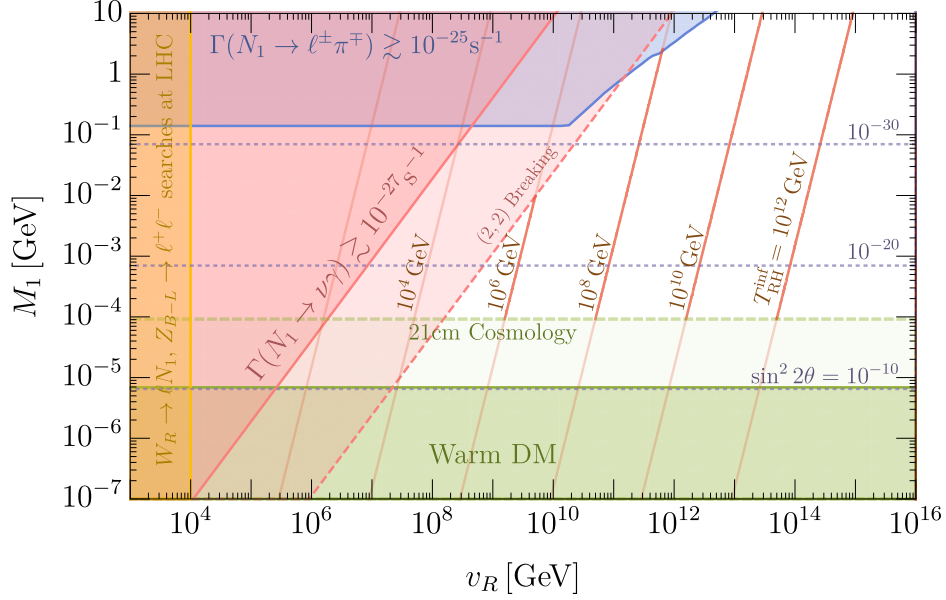


Figure 4. The parameter space for N_1 DM produced by freeze-in. The observed relic abundance occurs in the unshaded region for values of $T_{\text{RH}}^{\text{inf}}$ shown by the dashed red contours. Constraints from small scale structure are shown in green, with projections from future probes of small scale structure using the 21cm line in dashed green. In the blue region N_1 decays too rapidly via W_R to $\ell^\pm\pi^\mp$, and in the pink region N_1 decays too rapidly via $W_R - W_L$ mixing to $\nu\gamma$ when $SU(2)_L$ is broken by $(2, 1) + (1, 2)$ (solid) or by $(2, 2)$ (dashed). The decay via $W_R - W_L$ mixing to $\ell^+\ell^-\nu$ is weaker and not shown. The horizontal dashed blue lines show the limit (3.4) on the mixing angle of N_1 with active neutrinos. Collider searches for W_R exclude v_R below about 10 TeV, as shown in orange.

8 Conclusions

Since right-handed neutrinos N_i have no SM gauge interactions, it is plausible that one of them, N_1 , is sufficiently stable to make up dark matter. A theory containing N_i has three types of neutrino masses: Dirac masses, $(\nu_i N_j)$, and Majorana masses, $(\nu_i \nu_j)$ and $(N_i N_j)$. In general, these are described by three independent mass matrices. In this paper we have studied theories with a LR symmetry that forces the Majorana mass matrices for $(\nu_i \nu_j)$ and $(N_i N_j)$ to be proportional. In simple theories with the $SU(2)_R$ and $SU(2)_L$ gauge groups broken by doublet vacuum expectation values of strength v_R and v , the constant of proportionality is v^2/v_R^2 , whereas in the conventional LR theory, with scalar triplets and bidoublets, the constant of proportionality is $c v^2/v_R^2$, with $c \lesssim 1$.

At sufficiently high temperatures in the early universe, N_i are kept in thermal equilibrium via the $SU(2)_R$ gauge interactions. The initially thermal N_1 can account for the observed DM if they are subsequently diluted by decays of the initially thermal N_2 . We have shown that the (v_R, M_1) parameter space for this simple origin of DM is highly restricted, and indeed

bounded, as shown in Fig. 1. The allowed region is triangular with $v_R \simeq (10^8 - 3 \times 10^{12})$ GeV and $M_1 \simeq (2 \text{ keV} - 1 \text{ MeV})$ for $c = 1$. As c is reduced, the allowed region shrinks in size and shifts to lower values of (v_R, M_1) , disappearing entirely at $(10^6 \text{ GeV}, 2 \text{ keV})$ when $c \simeq 10^{-4}$.

Constraints that determine the lower bounds on M_1 and v_R are straightforward, arising from requirements that DM not be too warm and N_2 decays without disturbing nucleosynthesis. However, there is a third constraint, which leads to upper bounds on both M_1 and v_R , and is involved. In Appendix A we show that this DM scenario places constraints on the active neutrino masses in such a way that the mass of N_2 is determined by (4.9), and grows rapidly with v_R . Thus at large enough v_R , N_2 decays dominantly via W_R exchange; the requirement that this decay is slow enough to sufficiently dilute N_1 places an upper bound on $M_1 v_R$, as shown by the blue region of Fig. 1.

Observational probes of this N_1 DM, from relativistic freeze-out and dilution by N_2 decay, are shown in Fig. 2 for $c = 1$. The bulk of the (v_R, M_1) parameter space is at lower values of M_1 , leading to signals of warmness in large scale structure. Indeed, a significant portion of the parameter space can be observationally probed using 21 cm cosmology. A subdominant component of N_1 DM is produced non-thermally via the W_R beta decay $N_2 \rightarrow N_1 \ell^+ \ell^-$, producing N_1 that become non-relativistic at temperatures $\mathcal{O}(\text{eV})$ and are therefore hot. The size of this component is proportional to $(M_1 v_R)^2$ and, coincidentally, present limits on this hot DM component are close to the previously described limit on $M_1 v_R$ from too much N_1 DM. Indeed, the interesting case of N_2 decaying dominantly via W_R is already in tension with observation, and future CMB measurements will thoroughly probe this possibility. During the era of N_2 matter domination, density perturbations on small enough scales grow and could potentially lead to observable structures. Unfortunately, for pulsar timing arrays to see a signal in the region of reheat temperatures above the 4 MeV BBN bound, requires $M_1 > \text{MeV}$, which is excluded by insufficient dilution of N_1 .

Given that the decays of N_2 are out of thermal equilibrium, it is plausible that they lead to leptogenesis. We explore this in detail in a future publication [72], and here we simply observe that sufficient baryon asymmetry arises only if such decays are early enough, as shown by the dashed purple line in Fig. 2. A large fraction of the parameter space that allows leptogenesis can be probed by 21 cm cosmology.

The $SU(2) \times SU(2)_R \times U(1)_{B-L}$ gauge group studied in this paper provides an elegant setting for Higgs Parity [12–15], which correlates the SM parameters including the top quark and Higgs boson masses and the QCD coupling constant with the scale of $SU(2)_R$ breaking. The predicted top quark mass in this scheme is consistent with the experimentally preferred value of it for v_R in the range of $(10^9 - 10^{13})$ GeV, as shown in Fig. 3, which includes much of the range relevant for N_1 DM. As uncertainties in the Higgs mass and the QCD coupling are reduced in near future measurements, v_R is predicted within a factor of 10. It will be interesting to see whether the ranges of v_R for Higgs Parity and N_1 DM remain consistent. Precise measurements of the top quark mass at future linear colliders such as ILC can predict v_R with an accuracy of a few tens of percent. The range of v_R that gives precision gauge coupling unification is also shown in Fig. 3; remarkably it is consistent with Higgs Parity and

much of the range needed for N_1 DM. An important question is how easily the conditions for cosmological stability of N_1 can be implemented in a realistic $SO(10)$ theory of flavor.

In LR theories, if the reheat temperature after inflation is too low for W_R exchange to put N_i into thermal equilibrium, the N_1 DM abundance can be successfully generated by freeze-in, as shown by the solid red contours in Fig. 4. In this case the scale v_R is unconstrained, except by direct limits from LHC on the masses of W_R and Z_R . There are, however, strong limits on M_1 from warmness and from N_1 stability requirements.

Acknowledgement

We thank Bibhushan Shakya for useful discussion. This work was supported in part by the Director, Office of Science, Office of High Energy and Nuclear Physics, of the US Department of Energy under Contracts DE-AC02-05CH11231 (JD and LJH) and DE-SC0009988 (KH), as well as by the National Science Foundation under grants PHY-1316783 and PHY-1521446 (LJH).

A Neutrino mass relations

In this appendix, we show the constraints on the mass eigenvalues of the active neutrinos through the requirements of abundance and radiative stability of N_1 DM, together with cosmological bounds on the warmness of N_1 and the reheating temperature from N_2 decay. We remind the reader that we work in a mass basis for N_i , which have masses M_i . The states ν_i are related to N_i by LR symmetry, and are not necessarily mass eigenstates.

We first consider the case $M_3 > M_1$. Constraints on the Yukawa matrix y_{ij} , and lower bounds on M_1 and M_2 , then ensure that the seesaw mechanism is operative, so that the ν_i mass matrix is

$$m_{ij} = \delta_{ij} c \frac{v^2}{v_R^2} M_i - \sum_{k=1}^3 \frac{y_{ik} y_{jk}}{M_k} v^2 \quad (\text{A.1})$$

as in (2.5). We will demonstrate two claims:

Claim 1: The lightest eigenstate is aligned with ν_1 , with mass $m_1 \ll \sqrt{\Delta m_{\text{sol}}^2} \simeq 0.01$ eV.

Claim 2: The mass of N_2 is determined by $M_2 \simeq \mu (v_R/v)^2 c^{-1}$, where 0.01 eV $\lesssim \mu \lesssim 0.10$ eV. This is key to constraining the parameter space of frozen-out N_1 DM.

The stability of N_1 and N_2 require $|y_{1i}|, |y_{2i}| \ll 1$, as indicated by Eqs. (3.3) and (4.8), implying that the seesaw contributions from N_1 and N_2 exchange are both much less than

0.01 eV. Hence, to an excellent approximation, Eq. (A.1) can be written as

$$m_{ij} \simeq \begin{pmatrix} c \left(\frac{v}{v_R} \right)^2 M_1 - \frac{y_{13}^2}{M_3} v^2 & -\frac{y_{23}y_{13}}{M_3} v^2 & -\frac{y_{13}y_{33}}{M_3} v^2 \\ -\frac{y_{23}y_{13}}{M_3} & c \left(\frac{v}{v_R} \right)^2 M_2 - \frac{y_{23}^2}{M_3} v^2 & -\frac{y_{23}y_{33}}{M_3} v^2 \\ -\frac{y_{13}y_{33}}{M_3} v^2 & -\frac{y_{23}y_{33}}{M_3} v^2 & c \left(\frac{v}{v_R} \right)^2 M_3 - \frac{y_{33}^2}{M_3} v^2 \end{pmatrix}. \quad (\text{A.2})$$

Next we find that the entry m_{11} is much smaller than $\sqrt{\Delta m_{\text{sol}}^2}$:

$$\begin{aligned} c \left(\frac{v}{v_R} \right)^2 M_1 &\leq v^2 M_1 \left(\frac{1536\pi^3}{14M_2^5 M_{\text{Pl}}} \left(\frac{\pi^2 g_*(T_{\text{RH}})}{10} \right)^{1/2} \left(\frac{\rho_{\text{DM}}/s M_2}{1.6\frac{3}{4}M_1} \right)^2 \right)^{1/2} & (N_2 \text{ stability}) \\ &= 6 \times 10^{-6} \text{ eV} \left(\frac{24 \text{ GeV}}{M_2} \right)^{3/2} \left(\frac{g_*(T_{\text{RH}})}{10.9} \right)^{1/4}, & (\text{A.3}) \\ \frac{|y_{13}|^2}{M_3} v^2 &\leq \frac{M_1^2}{M_3} \sin^2 2\theta_1 \\ &\leq 8 \times 10^{-5} \text{ eV} \left(\frac{2 \text{ keV}}{M_1} \right)^4 \left(\frac{M_1/M_3}{1} \right). & (N_1 \text{ stability}) \end{aligned}$$

Now we argue that m_{13} is also negligible. The upper bound on $|y_{13}|$ of (3.3) from the stability of N_1 implies that m_{13} is non-negligible only if $|y_{33}|$ is large, such that $|y_{33}|^2 v^2 / M_3 \gg \sqrt{\Delta m_{\text{sol}}^2}$. To ensure that the observed sum of neutrino masses does not exceed 0.06–0.10 eV, m_{33} must be tuned such that $|y_{33}|^2 v^2 / M_3 \simeq c(v/v_R)^2 M_3$. However,

$$\begin{aligned} \frac{|y_{13}y_{33}|}{M_3} v^2 &\simeq \sqrt{c} \frac{|y_{31}| v^2}{v_R} & (\text{A.4}) \\ &\leq \sqrt{c} M_1 \sin \theta_1 \frac{v}{v_R} \\ &\leq M_1 \sin \theta_1 v \left(\frac{1536\pi^3}{14M_2^5 M_{\text{Pl}}} \left(\frac{\pi^2 g_*(T_{\text{RH}})}{10} \right)^{1/2} \left(\frac{\rho_{\text{DM}}/s M_2}{1.6\frac{3}{4}M_1} \right)^2 \right)^{1/4} & (N_2 \text{ stability}) \\ &\leq 2 \times 10^{-5} \text{ eV} \left(\frac{M_1}{2 \text{ keV}} \right)^{-2} \left(\frac{M_2}{24 \text{ GeV}} \right)^{-3/4}. & (N_1 \text{ stability}) \end{aligned}$$

Hence, from the lower bounds on $M_{1,2}$ we conclude that m_{13} is negligible.

The mass matrix of the active neutrinos is therefore approximately

$$m_{ij} \simeq \begin{pmatrix} 0 & -\frac{y_{23}y_{13}}{M_3}v^2 & 0 \\ -\frac{y_{23}y_{13}}{M_3} & c\left(\frac{v}{v_R}\right)^2 M_2 - \frac{y_{23}^2}{M_3}v^2 & -\frac{y_{23}y_{33}}{M_3}v^2 \\ 0 & -\frac{y_{23}y_{33}}{M_3}v^2 & c\left(\frac{v}{v_R}\right)^2 M_3 - \frac{y_{33}^2}{M_3}v^2 \end{pmatrix}. \quad (\text{A.5})$$

We put further constraints on the mass matrix by considering the two cases of M_3 : greater than or less than M_2 .

Case 1: $M_3 > M_2$

For this case, the entry m_{12} is negligible. This is because the upper bound on y_{32} is

$$|y_{23}|^2 \leq \frac{1}{\Gamma_0 M_{\text{Pl}}} \left(\frac{\pi^2 g_*(T_{\text{RH}})}{10} \right)^{1/2} \left(\frac{M_2 \rho_{\text{DM}}/s}{1.6 \frac{3}{4} M_1} \right)^2, \quad (N_2 \text{ stability})$$

$$\Gamma_0 \equiv \begin{cases} \frac{171/8}{1536\pi^3} \frac{M_2^3}{v^2} & M_2 < v \\ \frac{1}{8\pi} M_2 & M_2 > v, \end{cases} \quad (\text{A.6})$$

so that

$$|m_{12}| = \frac{|y_{13}y_{23}|v^2}{M_3} \quad (\text{A.7})$$

$$\leq \sin \theta_1 v \left(\frac{1}{\Gamma_0 M_{\text{Pl}}} \left(\frac{\pi^2 g_*(T_{\text{RH}})}{10} \right)^{1/2} \left(\frac{\rho_{\text{DM}}/s}{1.6 \frac{3}{4}} \right)^2 \right)^{1/2}.$$

(Stability of N_1 and N_2 , $M_3 > M_2$)

$$\leq 9 \times 10^{-10} \text{ eV} \left(\frac{M_1}{2 \text{ keV}} \right)^{-5/2} \left(\frac{M_2}{24 \text{ GeV}} \right)^{-3/2} \quad (\text{A.8})$$

Next we show that m_{23} is also small. The upper bound on y_{33} is

$$\begin{aligned}
|y_{33}|^2 &= \frac{M_3^2}{v^2} \left| \frac{m_{22} + \frac{y_{23}^2 v^2}{M_3}}{M_2} - \frac{m_{33}}{M_3} \right| && \text{(Rewriting } m_{33}\text{)} \\
&\leq \frac{M_3^2}{v^2} \left(\left| \frac{m_{22}}{M_2} \right| + \left| \frac{y_{23}^2 v^2}{M_2 M_3} \right| + \left| \frac{m_{33}}{M_3} \right| \right) && \text{(Triangle inequality)} \\
&\leq \frac{M_3^2}{v^2 M_2} \left(|m_{22}| + \left| \frac{y_{23}^2 v^2}{M_2} \right| + |m_{33}| \right) && (M_2 < M_3) \\
&\lesssim \frac{M_3^2}{v^2} \frac{\sum m_i}{M_2}. && \text{(Upper bound on } m_{22} \text{ and } m_{33}, N_2 \text{ stability)}
\end{aligned}$$

Hence, m_{23} is at most

$$|m_{23}| \leq v \sqrt{\left(\frac{1}{\Gamma_0 M_{\text{Pl}}} \left(\frac{\pi^2 g_*(T_{\text{RH}})}{10} \right)^{1/2} \left(\frac{M_2 \rho_{\text{DM}}/s}{1.6 \frac{3}{4} M_1} \right)^2 \right) \left(\frac{\sum m_i}{M_2} \right)}. \quad (\text{A.9})$$

Fig. 5 (left) shows the region where the right-side of Eq. (A.9) is greater than $\sqrt{\Delta m_{\text{sol}}^2}$ in the $M_1 - M_2$ plane. As can be seen, everywhere in the cosmologically allowed region $|m_{23}| \ll \sqrt{\Delta m_{\text{sol}}^2}$. In the active neutrino mass matrix, only m_{22} and m_{33} can be comparable to the observed neutrino masses; for $M_3 > M_2$ the ν_i basis is accurately the mass basis. The lightest active neutrino mass m_1 is much smaller than $\sqrt{\Delta m_{\text{sol}}^2}$, showing **Claim 1**.

The two heavier active neutrino masses (m_2, m_3) are simply given by

$$m_2 \simeq m_{22} = c \left(\frac{v}{v_R} \right)^2 M_2 - \frac{y_{23}^2 v^2}{M_3} \quad (\text{A.10})$$

$$m_3 \simeq m_{33} = c \left(\frac{v}{v_R} \right)^2 M_3 - \frac{y_{33}^2 v^2}{M_3} \quad (\text{A.11})$$

Furthermore,

$$\begin{aligned}
\frac{|y_{23}|^2 v^2}{M_3} &\leq \frac{|y_{23}|^2 v^2}{M_2} && (M_2 < M_3) \\
&\ll \sqrt{\Delta m_{\text{sol}}^2}. && (N_2 \text{ stability})
\end{aligned}$$

Therefore, we obtain **Claim 2**, with μ identified as m_2 , the mass of ν_2

$$M_2 \simeq m_2 \left(\frac{v_R}{v} \right)^2 \frac{1}{c}. \quad (\text{A.12})$$

Case 2: $M_3 < M_2$

We first show that $|y_{23}|^2 v^2 / M_3$ cannot be larger than the active neutrino mass by contradiction. Let us assume that $|y_{23}|^2 v^2 / M_3$ is larger than the active neutrino mass. Then to suppress m_{22} , we need

$$\frac{|y_{23}|^2 v^2}{M_3} \simeq c \left(\frac{v}{v_R} \right)^2 M_2. \quad (\text{A.13})$$

If $|y_{33}|$ is larger than $|y_{23}|$, $|y_{33}|^2 v^2 / M_3$ is also larger than the active neutrino mass and must be cancelled by $cM_3(v/v_R)^2$, which is impossible since $M_3 < M_2$. We conclude that $|y_{33}| < |y_{22}|$, which is used later.

Since $M_3 > M_1$, the case where N_3 decays after matter-radiation equality is excluded due to entropy production by the decay, or too much N_3 DM if N_3 is cosmologically stable. We thus assume that N_3 decays before matter-radiation equality.

Case 2-1: $M_2 < v$

Since $|y_{33}| < |y_{23}|$ and $|y_{13}|$ is small, the decay of N_3 by W_L exchange is determined by y_{23} . Then the decay rate of N_3 by W_R exchange is negligible. In fact, if N_3 decays dominantly by W_R exchange,

$$|y_{23}|^2 \frac{M_3^3}{v^2} < \frac{M_3^5}{v_R^4}. \quad (\text{A.14})$$

In this case, however,

$$\begin{aligned} \frac{|y_{23}|^2 v^2}{M_3} &\leq M_2 v^4 \left(\frac{1536\pi^3}{14M_2^5 M_{\text{Pl}}} \left(\frac{\pi^2 g_*(T_{\text{RH}})}{10} \right)^{1/2} \left(\frac{\rho_{\text{DM}}/s M_2}{1.6 \frac{3}{4} M_1} \right)^2 \right) \quad (N_2 \text{ stability, } M_2 > M_3) \\ &= 2 \times 10^{-7} \text{ eV} \left(\frac{M_2}{24 \text{ GeV}} \right)^{-2} \left(\frac{M_1}{2 \text{ keV}} \right)^{-2} \end{aligned} \quad (\text{A.15})$$

which is in contradiction. Thus N_3 decays dominantly by y_{32} .

In order for N_2 to be the diluter (by definition), it must be that

$$\begin{aligned} \frac{M_2}{\sqrt{\Gamma_{N_2}}} &> \frac{M_3}{\sqrt{\Gamma_{N_3}}}, & (\text{Dilution factor}) \\ \frac{M_2}{\sqrt{|y_{23}|^2 M_2^3}} &> \frac{M_3}{\sqrt{|y_{23}|^2 M_3^3}} & (\Gamma_{W_L} \propto y^2 M^3) \\ \Rightarrow M_3 &> M_2, & (\text{A.16}) \end{aligned}$$

which is a contradiction with our assumption that $M_3 < M_2$.

Case 2-2: $M_2 > v$

When $M_2 > v$, N_2 decays to ℓH via y_{2i} or beta-decays via W_R exchange. Both decay channels limit $|y_{23}|^2 v^2 / M_3$ to ensure N_2 is long-lived enough to provide dilution of N_1 .

From the decay via y_{2i} ,

$$\frac{|y_{23}|^2 v^2}{M_3} \leq \frac{v^2}{M_3} \frac{8\pi}{M_2 M_{\text{Pl}}} \left(\frac{\pi^2 g_*(T_{\text{RH}})}{10} \right)^{1/2} \left(\frac{\rho_{\text{DM}}/s M_2}{1.6 \frac{3}{4} M_1} \right)^2 \quad (N_2 \text{ stability})$$

To be compatible with our assumption that $|y_{23}|^2 v^2 / M_3 > m_1 + m_2 + m_3$, it is required that

$$\frac{M_3}{M_2} < \frac{8\pi v^2}{M_{\text{Pl}} \sum m_i} \left(\frac{\pi^2 g_*(T_{\text{RH}})}{10} \right)^{1/2} \left(\frac{\rho_{\text{DM}}/s}{1.6 \frac{3}{4} M_1} \right)^2 \quad (\text{A.17})$$

$$= 2 \times 10^{-9} \left(\frac{\sqrt{\Delta m_{\text{atm}}^2}}{\sum m_i} \right) \left(\frac{g_*(T_{\text{RH}})}{106.5} \right)^{1/2} \left(\frac{2 \text{ keV}}{M_1} \right)^2. \quad (\text{A.18})$$

The turquoise shaded region in Fig. 5 (**right**) violates this condition for the minimum value of $M_1 = 2 \text{ keV}$; larger M_1 enlarges the region. From the decay via W_R exchange,

$$\frac{|y_{23}|^2}{M_3} v^2 \leq M_2 \left(\frac{v}{v_R} \right)^2 \quad (\text{Since } c \leq 1)$$

$$\leq v^2 \left(\frac{1536\pi^3}{20M_2^3 M_{\text{Pl}}} \left(\frac{\pi^2 g_*(T_{\text{RH}})}{10} \right)^{1/2} \left(\frac{\rho_{\text{DM}}/s M_2}{1.6 \frac{3}{4} M_1} \right)^2 \right)^{1/2}. \quad (N_2 \text{ stability})$$

In the purple region of Fig. 5 (**right**), the inequality is less than $\sum m_i$, also for the minimum value of $M_1 = 2 \text{ keV}$.

There are additional constraints on M_2 and M_3 if N_3 decays after BBN. This occurs when

$$\Gamma_{N_3} \simeq (2 - 20) \times \frac{1}{1536\pi^3} \frac{M_3^3}{v^2} |y_{23}|^2 < (0.1 \text{ sec})^{-1}, \quad (\text{A.19})$$

where the coefficient depends on the kinematically available final states. If $M_3 > \text{few MeV}$, then the decay products of N_3 carry enough energy to dissociate light elements formed during BBN, altering their relic abundances (see [97] and references therein).¹⁰ If $M_3 \lesssim \text{MeV}$, the decay after BBN does not necessarily dissociate any light elements, but can still alter their relic abundance if N_3 is long-lived enough to induce a matter-dominated era before decaying. This occur when

$$\Gamma_{N_3} \lesssim \left(\frac{\pi^2 g_*}{10} \right)^{1/2} \frac{1}{M_{\text{Pl}}} \left(\frac{M_3}{M_1} \frac{\rho_{\text{DM}}}{s} \right)^2. \quad (\text{A.20})$$

These constraints are shown as the orange region of Fig. 5 (**right**), where we use the upper bound on $|y_{23}|$ from the stability of N_2 as discussed above and use the decay rate for $M_3 \gtrsim 2m_e$. For smaller M_3 , the actual decay rate is smaller and the abundance becomes larger. In the red shaded region of Fig. 5 (**right**), N_3 decays after it dominates the universe for the maximum value of $M_1 = M_3$; smaller M_1 enlarges the region. In the union of orange and red shaded regions, N_3 creates entropy after BBN, which is excluded since the baryon abundance at BBN and at CMB would differ. We see that no parameter region is then consistent with $|y_{23}|^2 v^2 / M_3$ being larger than the active neutrino mass, completing the proof.

¹⁰For $M_3 < 100 \text{ MeV}$ hadronic decays of N_3 are absent and the effect on BBN only comes from photo-dissociation which is effective for $T < 0.01 \text{ MeV}$. We find that N_3 decays below $T = 0.01 \text{ MeV}$ for $M_3 < 100 \text{ MeV}$.

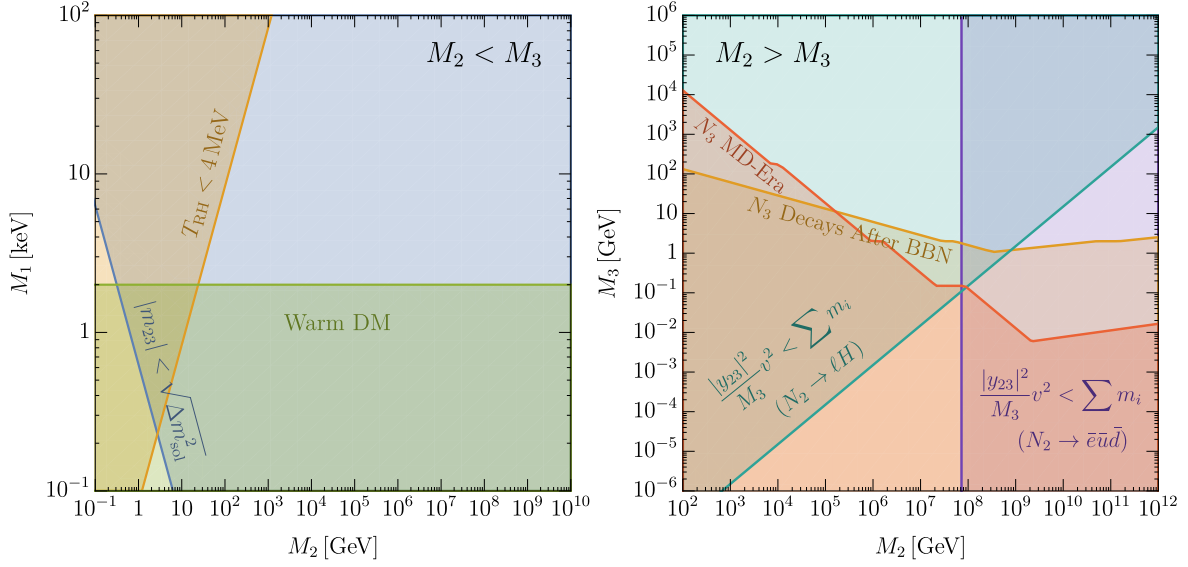


Figure 5. The right-handed neutrino mass parameter space showing the constraints which prove **Claim 1** and **Claim 2**. **Left:** $M_2 < M_3$ (Case 1) – the relation $M_2 = m_2(v_R/v)^2/c$ is guaranteed if $|m_{23}| < \sqrt{\Delta m_{\text{sol}}^2}$. Stability of N_2 ensures $|m_{23}| < \sqrt{\Delta m_{\text{sol}}^2}$ in **blue**, which encompasses all of the parameter space not excluded by the warmth of DM (**green**) or Big Bang Nucleosynthesis (**orange**). **Right:** $M_2 > M_3$ (Case 2) – the relation $M_2 = \mu(v_R/v)^2/c$, where $0.01 \text{ eV} \lesssim \mu \lesssim 0.10 \text{ eV}$, is guaranteed if $|y_{23}|^2 v^2/M_3 < \sum m_i$. Stability of N_2 ensures $|y_{23}|^2 v^2/M_3 < \sum m_i$ in the **purple** and **turquoise** regions which encompass all of the parameter space not excluded from N_3 decaying after Big Bang Nucleosynthesis (**orange**). N_3 disrupts Big Bang Nucleosynthesis from the energy released in its decays when $M_3 > 1 \text{ MeV}$ in the **orange** region, and from the entropy produced from its decays in the intersection of the **orange** and **red** regions.

Since $|y_{23}|^2 v^2/M_3$ is at the most as large as the active neutrino mass, with the upper bound on $|y_{13}|$ from the stability of N_1 , m_{23} is much smaller than the active neutrino mass. The active neutrino mass is almost 2 by 2, showing **Claim 1**.

The range of $cM_2(v/v_R)^2$ is constrained. It cannot be much larger than the active neutrino mass; since $|y_{23}|^2 v^2/M_3$ is at the most as large as the active neutrino mass, m_{22} cannot be fine-tuned to be small enough. If $cM_2(v/v_R)^2$ is much smaller than the active neutrino mass, $cM_3(v/v_R)^2$ is also small. Then the active neutrino mass matrix is dominantly given by the see-saw from M_3 , and two active neutrinos remain massless, which is in contradiction with observations. The only possibility is that $cM_2(v/v_R)^2$ is comparable to the active neutrino mass, showing **Claim 2**.

We next consider the case with $M_3 < M_1$. The term $c(v/v_R)^2 M_3$ is much smaller than the observed neutrino masses. The active neutrino mass matrix is dominantly given by the term $c(v/v_R)^2 M_2$ and the seesaw from N_3 , or a Dirac mass term with N_3 if $M_3 \ll 0.1 \text{ eV}$, and hence is essentially rank-2. The lightest active neutrino mass is much lighter than 0.01 eV .

If $c(v/v_R)^2 M_2$ is smaller than the observed active neutrino mass, the active neutrino mass matrix is essentially rank-1 and cannot explain the observed active neutrino mass. Thus, it is required that $c(v/v_R)^2 M_2 \gtrsim \mu$. It is possible that $c(v/v_R)^2 M_2 \gg \mu$ if it is cancelled by $|y_{23}|^2 v^2/M_3$. The constraint on the case with $c(v/v_R)^2 M_2 \gg \mu$ is obtained by interpreting Fig. 1 with c smaller than the actual value of c .

B A symmetry for the cosmological stability of N_1

For N_1 to make up dark matter, the mixing of active and sterile neutrinos must be very small to avoid limits on the radiative decay $N_1 \rightarrow \nu\gamma$, as shown in (3.4). Sufficient stability can be a natural if a symmetry forbids the $\ell N_1 H_L$ interaction in the effective theory (2.2), so that $y_{1i} = 0$. Any LR theory giving an effective theory below v_R with no interactions for N_i is particularly interesting: not only is N_1 cosmologically stable, but if N_2 has a mass significantly less than v_R , it is necessarily long-lived with a lifetime governed by W_R -mediated beta decay. In this case the allowed values of v_R and M_1 are correlated - it is necessary to be on the blue line of Fig. 1 rather than in the unshaded triangle. Furthermore, since N_2 has a 10% branching ratio to decay to N_1 , there is a component of DM that is hot, becoming non-relativistic around the eV era, with $\Delta N_{\text{eff}} \sim 0.1$ and $m_{\nu, \text{eff}} \sim 1.1$ eV. As described in Sec. 5.2, and shown in Fig. 2, this is close to present limits and will be discovered or refuted by CMB Stage IV [61].

For a LR model based on Higgs doublets $H_{L,R}$, such a symmetry must forbid the operator $\ell\bar{\ell} H_L H_R$, which leads to $\ell N H_L$, while allowing $\ell\bar{\ell} H_L^\dagger H_R^\dagger$, which yields the charged lepton Yukawa couplings $\ell\bar{e} H_L^\dagger$, as well as the Majorana mass operators $\ell\ell H_L H_L$ and $\bar{\ell}\bar{\ell} H_R H_R$. For example, this could be accomplished by a $Z_{4L} \times Z_{4R}$ symmetry with ℓ and H_L transforming as $(i, 1)$ and $(\bar{\ell}, H_R)$ as $(1, i)$. The operator $q\bar{q} H_L H_R$ or $q\bar{q} H_L^\dagger H_R^\dagger$ is inconsistent with this $Z_{4L} \times Z_{4R}$ symmetry, so that the down and/or up-type quark Yukawa couplings must be generated by a different set of doublets, $H_{L,R}^{(q)}$, with the effective theory below v_R containing the two doublets H_L and $H_L^{(q)}$. A weak-scale Nambu-Goldstone boson is avoided by introducing a soft breaking of the $Z_{4L} \times Z_{4R}$ symmetry via the mass operator $H_L^\dagger H_L^{(q)}$.

References

- [1] J. C. Pati and A. Salam, *Lepton Number as the Fourth Color*, *Phys. Rev. D* **10** (1974) 275.
- [2] R. Mohapatra and J. C. Pati, *A Natural Left-Right Symmetry*, *Phys. Rev. D* **11** (1975) 2558.
- [3] G. Senjanovic and R. N. Mohapatra, *Exact Left-Right Symmetry and Spontaneous Violation of Parity*, *Phys. Rev. D* **12** (1975) 1502.
- [4] H. Georgi, *The State of the Art—Gauge Theories*, *AIP Conf. Proc.* **23** (1975) 575.
- [5] H. Fritzsch and P. Minkowski, *Unified Interactions of Leptons and Hadrons*, *Annals Phys.* **93** (1975) 193.
- [6] H. Georgi and D. V. Nanopoulos, *Masses and Mixing in Unified Theories*, *Nucl. Phys. B* **159** (1979) 16.

- [7] T. Kibble, G. Lazarides and Q. Shafi, *Walls Bounded by Strings*, *Phys. Rev. D* **26** (1982) 435.
- [8] M. A. B. Beg and H. S. Tsao, *Strong P, T Noninvariances in a Superweak Theory*, *Phys. Rev. Lett.* **41** (1978) 278.
- [9] R. N. Mohapatra and G. Senjanovic, *Natural Suppression of Strong p and t Noninvariance*, *Phys. Lett.* **79B** (1978) 283.
- [10] K. S. Babu and R. N. Mohapatra, *CP Violation in Seesaw Models of Quark Masses*, *Phys. Rev. Lett.* **62** (1989) 1079.
- [11] K. S. Babu and R. N. Mohapatra, *A Solution to the Strong CP Problem Without an Axion*, *Phys. Rev.* **D41** (1990) 1286.
- [12] L. J. Hall and K. Harigaya, *Implications of Higgs Discovery for the Strong CP Problem and Unification*, *JHEP* **10** (2018) 130 [[1803.08119](#)].
- [13] D. Dunsky, L. J. Hall and K. Harigaya, *Higgs Parity, Strong CP, and Dark Matter*, *JHEP* **07** (2019) 016 [[1902.07726](#)].
- [14] L. J. Hall and K. Harigaya, *Higgs Parity Grand Unification*, *JHEP* **11** (2019) 033 [[1905.12722](#)].
- [15] D. Dunsky, L. J. Hall and K. Harigaya, *Dark Matter, Dark Radiation and Gravitational Waves from Mirror Higgs Parity*, *JHEP* **02** (2020) 078 [[1908.02756](#)].
- [16] S. Dodelson and L. M. Widrow, *Sterile-neutrinos as dark matter*, *Phys. Rev. Lett.* **72** (1994) 17 [[hep-ph/9303287](#)].
- [17] K. Perez, K. C. Y. Ng, J. F. Beacom, C. Hersh, S. Horiuchi and R. Krivonos, *Almost closing the ν MSM sterile neutrino dark matter window with NuSTAR*, *Phys. Rev.* **D95** (2017) 123002 [[1609.00667](#)].
- [18] X.-D. Shi and G. M. Fuller, *A New dark matter candidate: Nonthermal sterile neutrinos*, *Phys. Rev. Lett.* **82** (1999) 2832 [[astro-ph/9810076](#)].
- [19] F. Bezrukov, H. Hettmansperger and M. Lindner, *keV sterile neutrino Dark Matter in gauge extensions of the Standard Model*, *Phys. Rev.* **D81** (2010) 085032 [[0912.4415](#)].
- [20] S. Weinberg, *Baryon and Lepton Nonconserving Processes*, *Phys. Rev. Lett.* **43** (1979) 1566.
- [21] T. Yanagida, *Horizontal gauge symmetry and masses of neutrinos*, *Conf. Proc.* **C7902131** (1979) 95.
- [22] M. Gell-Mann, P. Ramond and R. Slansky, *Complex Spinors and Unified Theories*, *Conf. Proc.* **C790927** (1979) 315 [[1306.4669](#)].
- [23] P. Minkowski, *$\mu \rightarrow e\gamma$ at a Rate of One Out of 10^9 Muon Decays?*, *Phys. Lett.* **67B** (1977) 421.
- [24] R. N. Mohapatra and G. Senjanovic, *Neutrino Mass and Spontaneous Parity Nonconservation*, *Phys. Rev. Lett.* **44** (1980) 912.
- [25] M. Drewes et al., *A White Paper on keV Sterile Neutrino Dark Matter*, *JCAP* **1701** (2017) 025 [[1602.04816](#)].
- [26] K. Nandra et al., *The Hot and Energetic Universe: A White Paper presenting the science theme motivating the Athena+ mission*, [1306.2307](#).
- [27] V. Tatischeff et al., *The e-ASTROGAM gamma-ray space mission*, *Proc. SPIE Int. Soc. Opt. Eng.* **9905** (2016) 99052N [[1608.03739](#)].

- [28] A. Caputo, M. Regis and M. Taoso, *Searching for Sterile Neutrino with X-ray Intensity Mapping*, *JCAP* **2003** (2020) 001 [[1911.09120](#)].
- [29] E. Ma, *Verifiable radiative seesaw mechanism of neutrino mass and dark matter*, *Phys. Rev. D* **73** (2006) 077301 [[hep-ph/0601225](#)].
- [30] R. Essig, E. Kuflik, S. D. McDermott, T. Volansky and K. M. Zurek, *Constraining Light Dark Matter with Diffuse X-Ray and Gamma-Ray Observations*, *JHEP* **11** (2013) 193 [[1309.4091](#)].
- [31] L. Lavoura, *General formulae for $f(1) \rightarrow f(2)$ gamma*, *Eur. Phys. J. C* **29** (2003) 191 [[hep-ph/0302221](#)].
- [32] A. Greljo, D. J. Robinson, B. Shakya and J. Zupan, *$R(D^{(*)})$ from W' and right-handed neutrinos*, *JHEP* **09** (2018) 169 [[1804.04642](#)].
- [33] S. Tremaine and J. E. Gunn, *Dynamical Role of Light Neutral Leptons in Cosmology*, *Phys. Rev. Lett.* **42** (1979) 407.
- [34] A. Boyarsky, O. Ruchayskiy and D. Iakubovskiy, *A Lower bound on the mass of Dark Matter particles*, *JCAP* **0903** (2009) 005 [[0808.3902](#)].
- [35] D. Gorbunov, A. Khmel'nitskiy and V. Rubakov, *Constraining sterile neutrino dark matter by phase-space density observations*, *JCAP* **0810** (2008) 041 [[0808.3910](#)].
- [36] V. K. Narayanan, D. N. Spergel, R. Dave and C.-P. Ma, *Constraints on the mass of warm dark matter particles and the shape of the linear power spectrum from the Ly α forest*, *Astrophys. J.* **543** (2000) L103 [[astro-ph/0005095](#)].
- [37] V. Irsic et al., *New Constraints on the free-streaming of warm dark matter from intermediate and small scale Lyman- α forest data*, *Phys. Rev. D* **96** (2017) 023522 [[1702.01764](#)].
- [38] C. Yèche, N. Palanque-Delabrouille, J. Baur and H. du Mas des Bourboux, *Constraints on neutrino masses from Lyman-alpha forest power spectrum with BOSS and XQ-100*, *JCAP* **1706** (2017) 047 [[1702.03314](#)].
- [39] U. Seljak, A. Makarov, P. McDonald and H. Trac, *Can sterile neutrinos be the dark matter?*, *Phys. Rev. Lett.* **97** (2006) 191303 [[astro-ph/0602430](#)].
- [40] T. Asaka, M. Shaposhnikov and A. Kusenko, *Opening a new window for warm dark matter*, *Phys. Lett. B* **638** (2006) 401 [[hep-ph/0602150](#)].
- [41] K. Harigaya and M. Kawasaki, *QCD axion dark matter from long-lived domain walls during matter domination*, *Phys. Lett. B* **782** (2018) 1 [[1802.00579](#)].
- [42] M. Kawasaki, K. Kohri and N. Sugiyama, *Cosmological constraints on late time entropy production*, *Phys. Rev. Lett.* **82** (1999) 4168 [[astro-ph/9811437](#)].
- [43] M. Kawasaki, K. Kohri and N. Sugiyama, *MeV scale reheating temperature and thermalization of neutrino background*, *Phys. Rev. D* **62** (2000) 023506 [[astro-ph/0002127](#)].
- [44] T. Hasegawa, N. Hiroshima, K. Kohri, R. S. Hansen, T. Tram and S. Hannestad, *MeV-scale reheating temperature and thermalization of oscillating neutrinos by radiative and hadronic decays of massive particles*, *JCAP* **12** (2019) 012 [[1908.10189](#)].
- [45] K. Ichikawa, M. Kawasaki and F. Takahashi, *The Oscillation effects on thermalization of the neutrinos in the Universe with low reheating temperature*, *Phys. Rev. D* **72** (2005) 043522 [[astro-ph/0505395](#)].

- [46] P. F. de Salas, M. Lattanzi, G. Mangano, G. Miele, S. Pastor and O. Pisanti, *Bounds on very low reheating scenarios after Planck*, *Phys. Rev.* **D92** (2015) 123534 [[1511.00672](#)].
- [47] M. Nemevsek, G. Senjanovic and Y. Zhang, *Warm Dark Matter in Low Scale Left-Right Theory*, *JCAP* **1207** (2012) 006 [[1205.0844](#)].
- [48] D. Gorbunov and M. Shaposhnikov, *How to find neutral leptons of the ν MSM?*, *JHEP* **10** (2007) 015 [[0705.1729](#)].
- [49] J. Bond, G. Efstathiou and J. Silk, *Massive Neutrinos and the Large Scale Structure of the Universe*, *Phys. Rev. Lett.* **45** (1980) 1980.
- [50] H. Sato and F. Takahara, *Clustering of the Relic Neutrinos in the Expanding Universe*, *Progress of Theoretical Physics* **64** (1980) 2029.
- [51] F. R. Klinkhamer and C. Norman, *Massive Neutrinos and Galaxy Formation*, *Astrophys. J.* **243** (1981) L1.
- [52] I. Wasserman, *On the Linear Theory of Density Perturbations in a Neutrino Baryon Universe*, *Astrophys. J.* **248** (1981) 1.
- [53] K. A. Olive and M. S. Turner, *Cosmological Bounds on the Masses of Stable, Right-handed Neutrinos*, *Phys. Rev. D* **25** (1982) 213.
- [54] SDSS collaboration, *The Lyman-alpha forest power spectrum from the Sloan Digital Sky Survey*, *Astrophys. J. Suppl.* **163** (2006) 80 [[astro-ph/0405013](#)].
- [55] M. Viel, G. D. Becker, J. S. Bolton and M. G. Haehnelt, *Warm dark matter as a solution to the small scale crisis: New constraints from high redshift Lyman- α forest data*, *Phys. Rev.* **D88** (2013) 043502 [[1306.2314](#)].
- [56] PLANCK collaboration, *Planck 2018 results. VI. Cosmological parameters*, [1807.06209](#).
- [57] N. Banik, G. Bertone, J. Bovy and N. Bozorgnia, *Probing the nature of dark matter particles with stellar streams*, *JCAP* **1807** (2018) 061 [[1804.04384](#)].
- [58] J. B. Muñoz, C. Dvorkin and F.-Y. Cyr-Racine, *Probing the Small-Scale Matter Power Spectrum with Large-Scale 21-cm Data*, *Phys. Rev. D* **101** (2020) 063526 [[1911.11144](#)].
- [59] L. Feng, J.-F. Zhang and X. Zhang, *A search for sterile neutrinos with the latest cosmological observations*, *Eur. Phys. J.* **C77** (2017) 418 [[1703.04884](#)].
- [60] K. Abazajian et al., *CMB-S4 Science Case, Reference Design, and Project Plan*, [1907.04473](#).
- [61] CMB-S4 collaboration, *CMB-S4 Science Book, First Edition*, [1610.02743](#).
- [62] S. Böser, C. Buck, C. Giunti, J. Lesgourgues, L. Ludhova, S. Mertens et al., *Status of Light Sterile Neutrino Searches*, *Prog. Part. Nucl. Phys.* **111** (2020) 103736 [[1906.01739](#)].
- [63] CORE collaboration, *Exploring cosmic origins with CORE: Cosmological parameters*, *JCAP* **1804** (2018) 017 [[1612.00021](#)].
- [64] A. L. Erickcek and K. Sigurdson, *Reheating Effects in the Matter Power Spectrum and Implications for Substructure*, *Phys. Rev.* **D84** (2011) 083503 [[1106.0536](#)].
- [65] K.-Y. Choi and T. Takahashi, *New bound on low reheating temperature for dark matter in models with early matter domination*, *Phys. Rev.* **D96** (2017) 041301 [[1705.01200](#)].

- [66] E. F. Keane et al., *A Cosmic Census of Radio Pulsars with the SKA*, *PoS AASKA14* (2015) 040 [[1501.00056](#)].
- [67] J. A. Dror, H. Ramani, T. Trickle and K. M. Zurek, *Pulsar Timing Probes of Primordial Black Holes and Subhalos*, *Phys. Rev.* **D100** (2019) 023003 [[1901.04490](#)].
- [68] D. Croon, D. McKeen and N. Raj, *Gravitational microlensing by dark matter in extended structures*, [2002.08962](#).
- [69] Y. Bai, A. J. Long and S. Lu, *Tests of Dark MACHOs: Lensing, Accretion, and Glow*, [2003.13182](#).
- [70] E. W. Kolb and M. S. Turner, *The Early Universe*, vol. 69. 1990.
- [71] M. Fukugita and T. Yanagida, *Baryogenesis Without Grand Unification*, *Phys. Lett.* **B174** (1986) 45.
- [72] D. Dunsby, L. J. Hall and K. Harigaya, *Sterile Neutrino Dark Matter and Leptogenesis in Left-Right Higgs Parity*, [2007.12711](#).
- [73] R. T. Co, F. D’Eramo, L. J. Hall and D. Pappadopulo, *Freeze-In Dark Matter with Displaced Signatures at Colliders*, *JCAP* **1512** (2015) 024 [[1506.07532](#)].
- [74] J. A. Harvey and M. S. Turner, *Cosmological baryon and lepton number in the presence of electroweak fermion number violation*, *Phys. Rev.* **D42** (1990) 3344.
- [75] D. Buttazzo, G. Degrassi, P. P. Giardino, G. F. Giudice, F. Sala, A. Salvio et al., *Investigating the near-criticality of the Higgs boson*, *JHEP* **12** (2013) 089 [[1307.3536](#)].
- [76] PARTICLE DATA GROUP collaboration, *Review of Particle Physics*, *Phys. Rev. D* **98** (2018) 030001.
- [77] M. Cepeda et al., *Report from Working Group 2*, *CERN Yellow Rep. Monogr.* **7** (2019) 221 [[1902.00134](#)].
- [78] G. P. Lepage, P. B. Mackenzie and M. E. Peskin, *Expected Precision of Higgs Boson Partial Widths within the Standard Model*, [1404.0319](#).
- [79] TLEP DESIGN STUDY WORKING GROUP collaboration, *First Look at the Physics Case of TLEP*, *JHEP* **01** (2014) 164 [[1308.6176](#)].
- [80] K. Seidel, F. Simon, M. Tesar and S. Poss, *Top quark mass measurements at and above threshold at CLIC*, *Eur. Phys. J. C* **73** (2013) 2530 [[1303.3758](#)].
- [81] T. Horiguchi, A. Ishikawa, T. Suehara, K. Fujii, Y. Sumino, Y. Kiyo et al., *Study of top quark pair production near threshold at the ILC*, [1310.0563](#).
- [82] Y. Kiyo, G. Mishima and Y. Sumino, *Strong IR Cancellation in Heavy Quarkonium and Precise Top Mass Determination*, *JHEP* **11** (2015) 084 [[1506.06542](#)].
- [83] M. Beneke, Y. Kiyo, P. Marquard, A. Penin, J. Piclum and M. Steinhauser, *Next-to-Next-to-Next-to-Leading Order QCD Prediction for the Top Antitop S-Wave Pair Production Cross Section Near Threshold in e^+e^- Annihilation*, *Phys. Rev. Lett.* **115** (2015) 192001 [[1506.06864](#)].
- [84] *The International Linear Collider Technical Design Report - Volume 2: Physics*, [1306.6352](#).

- [85] T. G. Rizzo and G. Senjanovic, *Grand Unification and Parity Restoration at Low-energies. 2. Unification Constraints*, *Phys. Rev. D* **25** (1982) 235.
- [86] F. Siringo, *Grand unification in the minimal left-right symmetric extension of the standard model*, *Phys. Part. Nucl. Lett.* **10** (2013) 94 [[1208.3599](#)].
- [87] Y. Kawamura, *Gauge symmetry Reduction from the extra space S^1/Z_2* , *Prog. Theor. Phys.* **103** (2000) 613 [[hep-ph/9902423](#)].
- [88] Y. Kawamura, *Triplet doublet splitting, proton stability and extra dimension*, *Prog. Theor. Phys.* **105** (2001) 999 [[hep-ph/0012125](#)].
- [89] G. Altarelli and F. Feruglio, *$SU(5)$ grand unification in extra dimensions and proton decay*, *Phys. Lett.* **B511** (2001) 257 [[hep-ph/0102301](#)].
- [90] L. J. Hall and Y. Nomura, *Gauge unification in higher dimensions*, *Phys. Rev. D* **64** (2001) 055003 [[hep-ph/0103125](#)].
- [91] A. Hebecker and J. March-Russell, *A Minimal $S^1/(Z_2 \times Z'_2)$ orbifold GUT*, *Nucl. Phys.* **B613** (2001) 3 [[hep-ph/0106166](#)].
- [92] L. J. Hall, Y. Nomura, T. Okui and D. Tucker-Smith, *$SO(10)$ unified theories in six-dimensions*, *Phys. Rev. D* **65** (2002) 035008 [[hep-ph/0108071](#)].
- [93] S. Biermann, A. Mütter, E. Parr, M. Ratz and P. K. Vaudrevange, *Discrete remnants of orbifolding*, *Phys. Rev. D* **100** (2019) 066030 [[1906.10276](#)].
- [94] J. Heeck and D. Teresi, *Cold keV dark matter from decays and scatterings*, *Phys. Rev.* **D96** (2017) 035018 [[1706.09909](#)].
- [95] ATLAS collaboration, *Search for a heavy charged boson in events with a charged lepton and missing transverse momentum from pp collisions at $\sqrt{s} = 13$ TeV with the ATLAS detector*, *Phys. Rev.* **D100** (2019) 052013 [[1906.05609](#)].
- [96] ATLAS collaboration, *Search for high-mass dilepton resonances using 139 fb⁻¹ of pp collision data collected at $\sqrt{s} = 13$ TeV with the ATLAS detector*, *Phys. Lett.* **B796** (2019) 68 [[1903.06248](#)].
- [97] M. Kawasaki, K. Kohri and T. Moroi, *Big-Bang nucleosynthesis and hadronic decay of long-lived massive particles*, *Phys. Rev.* **D71** (2005) 083502 [[astro-ph/0408426](#)].